PD CEN/CLC/TR 17603-31-07:2021

BSI Standards Publication

Space Engineering — Thermal design handbook

Part 7: Insulations

Documents
Document Sharing Hub

Full document details: PD CEN/CLC/TR 17603-31-07:2021

National foreword

This Published Document is the UK implementation of CEN/CLC/TR 17603-31-07:2021.

The UK participation in its preparation was entrusted to Technical Committee ACE/68, Space systems and operations.

A list of organizations represented on this committee can be obtained on request to its committee manager.

Contractual and legal considerations

This publication has been prepared in good faith, however no representation, warranty, assurance or undertaking (express or implied) is or will be made, and no responsibility or liability is or will be accepted by BSI in relation to the adequacy, accuracy, completeness or reasonableness of this publication. All and any such responsibility and liability is expressly disclaimed to the full extent permitted by the law.

This publication is provided as is, and is to be used at the recipient's own risk.

The recipient is advised to consider seeking professional guidance with respect to its use of this publication.

This publication is not intended to constitute a contract. Users are responsible for its correct application.

This publication is not to be regarded as a British Standard.

© The British Standards Institution 2021
Published by BSI Standards Limited 2021

ISBN 978 0 539 16981 2

ICS 49.140

Compliance with a Published Document cannot confer immunity from legal obligations.

This Published Document was published under the authority of the Standards Policy and Strategy Committee on 31 August 2021.

Amendments/corrigenda issued since publication

Date	Text affected

Documents
Document Sharing Hub

Full document details: PD CEN/CLC/TR 17603-31-07:2021

TECHNICAL REPORT

RAPPORT TECHNIQUE

TECHNISCHER BERICHT

CEN/CLC/TR 17603-31-07

August 2021

ICS 49.140

English version

Space Engineering - Thermal design handbook - Part 7: Insulations

Ingénierie spatiale - Manuel de conception thermique - Partie 7 : Isolations

Raumfahrttechnik - Handbuch für thermisches Design - Teil 7: Isolationen

This Technical Report was approved by CEN on 21 June 2021. It has been drawn up by the Technical Committee CEN/CLC/JTC 5.

CEN and CENELEC members are the national standards bodies and national electrotechnical committees of Austria, Belgium, Bulgaria, Croatia, Cyprus, Czech Republic, Denmark, Estonia, Finland, France, Germany, Greece, Hungary, Iceland, Ireland, Italy, Latvia, Lithuania, Luxembourg, Malta, Netherlands, Norway, Poland, Portugal, Republic of North Macedonia, Romania, Serbia, Slovakia, Slovenia, Spain, Sweden, Switzerland, Turkey and United Kingdom.

CEN-CENELEC Management Centre:
Rue de la Science 23, B-1040 Brussels

© 2021 CEN/CENELEC All rights of exploitation in any form and by any means reserved worldwide for CEN national Members and for CENELEC Members.

AVA Documents Document Sharing Hub

Full document details: PD CEN/CLC/TR 17603-31-07:2021

Table of contents

European Foreword **14**

1 Scope **15**

2 References **16**

3 Terms, definitions and symbols **17**

3.1 Terms and definitions 17

3.2 Abbreviated terms 17

3.3 Symbols 17

4 Foams **22**

4.1 General 22

4.2 Inorganic foams 25

4.3 Organic foams 31

4.3.2 Thermal properties of organic foams 32

4.3.3 Mechanical properties of organic foams 35

4.3.4 Data on commercially available foams 53

5 Fibrous insulations **64**

5.1 General 64

5.2 Bulks 66

5.3 Blankets and felts 77

5.4 Papers 102

6 Multilayer insulations **108**

6.1 General 108

6.1.1 Fundamental concepts concerning MLI performance 109

6.1.2 Failure modes 111

6.1.3 Heat transfer through an MLI 111

6.1.4 Cost 118

6.2 Radiation shields 118

6.2.1 Aluminium foils and aluminium coated plastic films 118

6.2.2 Gold foils and gold coated plastic films 119

6.2.3 Silver coated plastic films 119

Documents
Document Sharing Hub

Full document details: PD CEN/CLC/TR 17603-31-07:2021

6.2.4 Operating temperature ranges 119
6.2.5 Normally used plastic films 120
6.3 Emittance of metallic foils 120
6.4 Emittance of metallized films 135
6.5 Absorptance of metallic foils 148
6.6 Radiation shields. miscellaneous properties 165
6.7 Radiation shields. measurement of the coating thickness 180
6.8 Spacers 183
6.8.1 Multiple-resistance spacers 184
6.8.2 Point-contact spacers 184
6.8.3 Superfloc 184
6.8.4 Single-component MLI 185
6.8.5 Composite spacers 185
6.8.6 One-dimensional heat flow through an mli with absorbing and scattering spacers 187
6.9 Spacers. miscellaneous properties 189
6.10 Complete systems 208
6.11 Normal heat transfer 209
6.12 Lateral heat transfer 251
6.13 Effect of singularities 257
6.13.1 Joints 257
6.13.2 Stitches and patches 269
6.14 Effect of evacuating holes 272
6.15 Effect of mechanical damage 276
6.16 Effect of inner gas pressure 277
6.17 Evacuation 285
6.17.1 Interstitial pressure during rapid evacuation 285
6.17.2 Interstitial pressure in outgas controlled situations 292
6.17.3 Self-pumping multilayer insulations 301

Bibliography 319

Figures

Figure 4-1: Resin thermal conductivity 23
Figure 4-2 : Gas thermal conductivity 23
Figure 4-3: Radiation thermal conductivity 24
Figure 4-4: Thermal conductivity, k, of several ceramic foams as a function of arithmetic mean temperature, T_m 26

Documents
Document Sharing Hub
Full document details: PD CEN/CLC/TR 17603-31-07:2021

Figure 4-5: Linear thermal expansion, $\Delta L/L$, of several ceramic foams as a function of temperature, T.....27

Figure 4-6: Temperature evolution of the hot and cold faces of several pieces of Zircon foam. Solid line: T_H, hot face. Dashed line: T_C, cold face.....28

Figure 4-7: Thermal conductivity k, of polyurethane foams vs. arithmetic mean temperature, T_m.....32

Figure 4-8: Thermal conductivity, k, of cryopumped polystyrene foams.....33

Figure 4-9: Thermal conductivity, k, vs. arithmetic mean temperature, T_m, of a polyurethane foam in the proximity of the condensation temperature of the filling gas.....34

Figure 4-10: Linear thermal expansion, $\Delta L/L$, of several organic foams as a function of temperature, T.....35

Figure 4-11: Ultimate tensile strength, of several foams as a function of temperature, T. 36

Figure 4-12: Ultimate shear strength, τ_{ult}, of several foams as a function of temperature, T.....37

Figure 4-13: Tensile stress, σ, vs. strain, δ, for several polyurethane foams at 76, 195 and 300 K.....46

Figure 4-14: Modulus of Elasticity-tensile-E, as a function of density, ρ, for several organic foams.....46

Figure 4-15: Ultimate tensile strength, σ_{ult}, as a function of density, ρ, for several organic foams.....47

Figure 4-16: Compressive stress, s, vs, strain, d, for several organic foams at 76, 195 and 300 K.....47

Figure 4-17: Modulus of Elasticity-tensile-E, as a function of density, ρ, for several organic foams.....48

Figure 4-18: Proportional limit-compressive-σ, as a function of density, ρ, for several organic foams.....49

Figure 4-19: Ultimate tensile strength, σ_{ult}, and Modulus of Elasticity-tensile-E, as functions of temperature, T.....50

Figure 4-20: Ultimate compressive strength, σ_{ult}, and Modulus of Elasticity-compressive-E, as functions of temperature, T.....51

Figure 4-21: Ultimate compressive strength, σ_{ult}, as a function of temperature, T. 52

Figure 4-22: Ultimate block shear strength, τ_{ult}, and Modulus of Elasticity-shear block-E, as functions of temperature, T. 53

Figure 4-23: Strain, δ, vs. compressive stress, σ, of Fiberfill Structural Foams. 62

Figure 4-24: Dielectric constant, ε_r, and dissipation factor, D, vs. frequency, f. Stycast 1090. 62

Figure 5-1: Thermal conductivity, k, vs. mean temperature, T_m, for several fibrous insulations. From Glasser et al. (1967) [23]. 65

Figure 5-2: Thermal conductivity, k, of B & W Kaowool bulk vs. mean temperature, Tm.....74

Figure 5-3: Thermal conductivity, k, of Carborundum Fiberfrax bulk and washed fibers vs. mean temperature, Tm. 74

Figure 5-4: Temperature differential, $T_H - T_C$, vs. mean temperature of the hot face, T_H,.....75

Documents
Document Sharing Hub

Full document details: PD CEN/CLC/TR 17603-31-07:2021

Figure 5-5: Temperature differential, T_H–T_C, vs. mean temperature of the hot face, T_H,.....75

Figure 5-6: Temperature differential, T_H–T_C, vs. mean temperature of the hot face, T_H,.....76

Figure 5-7: Temperature differential, T_H–T_C, vs. mean temperature of the hot face, T_H for different values of the insulation thickness, *t*. Fiberfrax washed fiber, ρ = 96 kg.m^{-3}.....76

Figure 5-8: Sound absorption coefficient, α, as a function of frequency, *f*, for B & W Kaowool blanket 2,54x10^{-2} m thick.....86

Figure 5-9: Sound absorption coefficient, α, as a function of frequency, *f*, for the following Fiberfrax products:.....86

Figure 5-10: Air permeability across B & W Kaowool blankets.....87

Figure 5-11: Air permeability across Carborundum Fiberfrax blankets.....88

Figure 5-12: Thermal conductivity, *k*, of B & Kaowool blankets vs. mean temperature, T_m.....88

Figure 5-13: Thermal conductivity, *k*, of Fiberfrax blankets vs. mean temperature, T_m.....89

Figure 5-14: Temperature differential, T_H–T_C, vs. temperature of the hot face T_H for different values of the blanket thickness, *t*. Fiberfrax Lo-Con Blanket & felt, ρ = 64 kg.m^{-3}.....89

Figure 5-15: Temperature differential, T_H–T_C, vs. temperature of the hot face, T_H, ...90

Figure 5-16: Sound absorption coefficient, α, as a function of frequency, *f*, for J-M Microlite Standard and Silicone Binder. 91

Figure 5-17: Calculated specific heat, *c*, as a function of temperature, *T*, for J.M Dyna-Quartz 91

Figure 5-18: Thermal conductivity, *k*, of J-M Micro-Quartz felt vs. mean temperature, T_m.....93

Figure 5-19: Thermal conductivity, *k*, of J-M Dyna-Quartz vs. mean temperature, T_m. 93

Figure 5-20: Thermal conductivity, *k*, of J-M Microlite "AA" and "B" vs. mean temperature, T_m.....94

Figure 5-21: Compressive stress, σ, vs. compressive strain, δ, for J-M Dyna-Quartz. 94

Figure 5-22: Linear Shrinkage, *LS*, and Total Weight Loss, *TWL*, of J-M Micro-Quartz Felt as a function of temperature, *T*. 95

Figure 5-23: Calculated specific heat, *c*, as a function of temperature, *T*, for several J-M insulations. 96

Figure 5-24: Thermal conductivity, *k*, of J-M Min-K 1301 vs. mean temperature, T_m. Numbers on curves indicate the density in kg.m^{-3}. 97

Figure 5-25: Influence of ambient pressure on the variation of thermal conductivity, *k*, of J-M Min-K 1301 vs. mean temperature, T_m, for several filling gases. 97

Figure 5-26: Thermal conductivity, *k*, of J-M Min-K 1301 vs. mean temperature, T_m, for different values of thickness, *t*. 98

Figure 5-27: Thermal conductivity, *k*, of J-M Min-K 2000 vs. mean temperature, T_m. 98

Figure 5-28: Influence of ambient pressure on the variation of thermal conductivity, *k*, of J-M Min-K 2000 vs. mean temperature, T_m, for several filling gases. 99

Figure 5-29: Thermal conductivity, *k*, of J-M Min-K 2000 vs. mean temperature, T_m, for different values of thickness, *t*. 99

Documents
Document Sharing Hub

Full document details: PD CEN/CLC/TR 17603-31-07:2021

Figure 5-30: Thermal conductivity, k, of J-M unbounded B-Fiber batt vs. mean temperature, T_m. 100

Figure 5-31: Thermal conductivity, k, of J-M Micro-Fibers felt Type "E" vs. mean temperature, T_m. 100

Figure 5-32: Compressive stress, σ, vs. compressive strain, δ, for J-M Min-K 1301. Numbers on curves indicate the density in kg.m^{-3}. 101

Figure 5-33: Compressive stress, σ, vs. compressive strain, δ, for J-M Min-K 2000. 101

Figure 5-34: Thermal conductivity, k, of B & W Kaowool, Carborundum Fiberfrax 970 paper, and Fiberfrax Hi-Fi 660 paper vs. mean temperature, T_m. 106

Figure 5-35: Temperature differential, $T_H - T_C$, vs. temperature of the hot face, T_H, for different values of the paper thickness, t. Fiberfrax 970 paper, ρ = 160 kg.m^{-3} 106

Figure 5-36: Temperature differential, $T_H - T_C$, vs. temperature of the hot face, T_H, for different values of the paper thickness, t. Fiberfrax Hi-Fi 660 paper. 107

Figure 5-37: Thermal reflectance, ρ, of Fiberfrax 970-J paper vs. mean temperature, T_m. 107

Figure 6-1: Effective thermal conductivity, k_{eff}, of multilayer insulations as compared with other insulation materials. From Glaser et al. (1967) [23]. 109

Figure 6-2: Effective thermal conductivity, keff, of several multilayer insulation systems as a function of the characteristic temperature, T. Calculated by the compiler. 116

Figure 6-3: Summary of data concerning hemispherical total emittance, ε, of Aluminium foils and thin sheets as a function of temperature, T. 121

Figure 6-4: Summary of data concerning hemispherical total emittance, ε, of Copper as a function of temperature, T. 122

Figure 6-5: Hemispherical total emittance, ε, of Copper as a function of temperature, T. 123

Figure 6-6: Hemispherical total emittance, ε, of Copper as a function of temperature, T. 124

Figure 6-7: Hemispherical total emittance, ε, of Gold vs. temperature, T. 125

Figure 6-8: Hemispherical total emittance, ε, of Molybdenum vs. temperature, T. 126

Figure 6-9: Hemispherical total emittance, ε, of Nickel vs. temperature, T. 128

Figure 6-10: Hemispherical total emittance, ε, of oxidized Nickel as a function of temperature, T. 129

Figure 6-11: Normal total emittance, ε', of Nickel as a function of temperature, T. 130

Figure 6-12: Normal total emittance, ε', of Inconel as a function of temperature, T. 131

Figure 6-13: Normal total emittance, ε', of Inconel X as a function of temperature, T. 132

Figure 6-14: Hemispherical total emittance, ε, of Platinum as a function of temperature, T. 133

Figure 6-15: Hemispherical total emittance, ε, of Silver as a function of temperature, T. 134

Figure 6-16: Hemispherical total emittance, ε, of Aluminized Mylar as a function of coating thickness, t_c. 136

Figure 6-17: Hemispherical total emittance, ε, of Copper on Mylar as a function of coating thickness, t_c. 137

Documents
Document Sharing Hub

Full document details: PD CEN/CLC/TR 17603-31-07:2021

Figure 6-18: Hemispherical total emittance, ε, of Goldized Mylar as a function of coating thickness, t_c.....138
Figure 6-19: Hemispherical total emittance, ε, of Gold on Double Aluminized Mylar as a function of Gold thickness, t_c. 139
Figure 6-20: Hemispherical total emittance, ε, of Silvered Mylar as a function of coating thickness, t_c. 140
Figure 6-21: Hemispherical total emittance, ε, of Silvered Mylar overcoated with Silicon Monoxide as a function of Silver thickness, t_c. 141
Figure 6-22: Hemispherical total emittance, ε, of Aluminized Kapton as a function of temperature, T.....143
Figure 6-23: Hemispherical total emittance, ε, of Aluminized Kapton as a function of coating thickness, t_c, for T = 300 K. 144
Figure 6-24: Hemispherical total emittance, ε, of Aluminized Kapton as a function of coating thickness, t_c, for T = 400 K. 145
Figure 6-25: Hemispherical total emittance, ε, of Silgle-Goldized Kapton as a function of temperature, T.....146
Figure 6-26: Hemispherical total emittance, ε, of Silgle-Silvered Kapton as a function of temperature, T.....147
Figure 6-27: Normal spectral absorptance, α'_λ, of Aluminium as a function of wavelength, λ. 148
Figure 6-28: Normal solar absorptance, α_s, of Aluminium as a function of temperature, T.....149
Figure 6-29: Normal spectral absorptance, α'_λ, of Copper as a function of wavelength λ....150
Figure 6-30: Normal solar absorptance, α_s, of Copper as a function of temperature T.....151
Figure 6-31: Normal spectral absorptance, α'_λ, of Gold as a function of wavelengthλ 152
Figure 6-32: Normal solar absorptance, α_s, of Gold as a function of temperature T. 153
Figure 6-33: Normal spectral absorptance, α'_λ, of Molybdenum as a function of wavelength λ. 154
Figure 6-34: Normal solar absorptance, α_s, of Molybdenum as a function of temperature T 155
Figure 6-35: Normal spectral absorptance, α'_λ, of Nickel as a function of wavelength λ.....156
Figure 6-36: Normal solar absorptance, α_s, of Nickel as a function of temperature, T.....158
Figure 6-37: Normal spectral absorptance, α'_λ, of Incoel as a function of wavelength λ.....159
Figure 6-38: Normal solar absorptance, α_s, of Incoel as a function of the temperature, T, to which samples had been previously heated. 160
Figure 6-39: Normal spectral absorptance, α'_λ, of Platinum as a function of wavelengthλ. 161
Figure 6-40: Normal solar absorptance, α_s, of Platinum as a function of temperature, T.....162
Figure 6-41: Normal spectral absorptance, α'_λ, of Silver as a function of wavelength, λ. 163
Figure 6-42: Normal solar absorptance, α_s, of Silver as a function of temperature, T. 164

Documents
Document Sharing Hub
Full document details: PD CEN/CLC/TR 17603-31-07:2021

Figure 6-43: Linear thermal expansion, $\Delta L/L$, of two nominally identical specimens of 6,35x10^{-6} m thick Mylar Double-Goldized as a function of temperature, T.....172

Figure 6-44: Linear thermal expansion, $\Delta L/L$ of 6,35x10^{-6} - 7,62x10^{-6} m thick Kapton Double-Goldized, with Dacron Flocking, as a function of temperature, T.....173

Figure 6-45: Coating thickness, t_c, given by several methods, compared with that gives by the electrical resistance method, $t_{c\Omega}$.....181

Figure 6-46: Thickness, $t_{c\Omega}$, of metallic coatings as a function of film electrical resistance, R. Calculated by the compiler.....183

Figure 6-47: Apparent emittance, ε_a, of a gray V-Groove as a function of surface emittance, ε, illustrating the effect of embossing or crinkling on the optical properties of the shield. Calculated by the compiler. 186

Figure 6-48: Effective thermal conductivity, k_{eff}, of several fibrous spacers as a function of mean temperature, T.....199

Figure 6-49: Effective thermal conductivity, k_{eff}, of Fiber-glass batting as a function of Nitrogen gas pressure, p. 200

Figure 6-50: Effective thermal conductivity, k_{eff}, of Dexiglas as a function of warm-boundary temperature, T_H. 201

Figure 6-51: Effective thermal conductivity, k_{eff}, of Tissuglas as a function of warm-boundary temperature, T_H. 202

Figure 6-52: Effective thermal conductivity, k_{eff}, of Refrasil as a function of warm-boundary temperature, T_H. 203

Figure 6-53: Effective thermal conductivity, k_{eff}, of several spacer materials as a function of bulk density, ρ. 204

Figure 6-54: Specific Heat, c, of several spacer materials as a function of temperature, T.....205

Figure 6-55: Effective thermal conductivity, k_{eff}, and product of apparent density and effective thermal conductivity, ρk_{eff}, vs. the number of radiation shields per unit thickness, N/t.....211

Figure 6-56: Compressive mechanical load, P, on the multilayer insulation vs. the number of radiation shields per unit thickness, N/t. 212

Figure 6-57: Effective thermal conductivity, k_{eff}, and product of apparent density and effective thermal conductivity, ρk_{eff}, vs. the number of radiation shields per unit thickness, N/t.....215

Figure 6-58: Effective thermal conductivity, k_{eff}, as a function of the characteristic temperature, T.....216

Figure 6-59: Heat flux, Q/A, across a single-aluminized Mylar, crinkled, MLI on different substrate plates, as a function of the number of radiation shields, N. T = 195 K, p = 2 x 10^{-3} Pa. N/t = 1100 $\pm$ 200 m^{-1}.....217

Figure 6-60: Effective thermal conductivity, k_{eff}, of a single-aluminized Mylar, crinkled, MLI on two different substrate plates, as a function of the number of radiation shields, N.....218

Figure 6-61: Heat flux, Q/A, across a single-aluminized Mylar, crinkled, MLI on different substrate plates, as a function of the pressure, p. T = 195 K. Layer density, N/t = 1100 $\pm$ 200 m^{-1} in any case.....219

Documents
Document Sharing Hub

Full document details: PD CEN/CLC/TR 17603-31-07:2021

Figure 6-62: Effective thermal conductivity, k_{eff}, and product of apparent density and effective thermal conductivity, ρk_{eff}, vs. the number of radiation shields per unit thickness, *N/t*. 220

Figure 6-63: Effective thermal conductivity, k_{eff}, as a function of the characteristic temperature, *T*. 221

Figure 6-64: Effective thermal conductivity, k_{eff}, and product of apparent density and effective thermal conductivity, ρk_{eff}, vs. the number of radiation shields per unit thickness, *N/t*. 222

Figure 6-65: Compressive mechanical load, *P*, on the multilayer insulation vs. the number of radiation shields per unit thickness, *N/t*. 223

Figure 6-66: Effective thermal conductivity, k_{eff}, and product of apparent density and effective thermal conductivity, ρk_{eff}, vs. number of radiation shields per unit thickness, *N/t*. 224

Figure 6-67: Compressive mechanical load, *P*, on the multilayer insulation vs. the number of radiation shields per unit thickness, *N/t*. 225

Figure 6-68: Effective thermal conductivity, k_{eff}, as a function of the characteristic temperature, *T*. 225

Figure 6-69: Effective thermal conductivity, k_{eff}, and product of apparent density and effective thermal conductivity, ρk_{eff}, vs. the number of radiation shields per unit thickness, *N/t*. Arrows in curves indicate whether the system is being loaded or unloaded. 228

Figure 6-70: Compressive mechanical load, *P*, on the multilayer insulation vs. the number of radiation shields per unit thickness, *N/t*. 229

Figure 6-71: Effective thermal conductivity, k_{eff}, as a function of the characteristic temperature, *T*. 229

Figure 6-72: Effective thermal conductivity, k_{eff}, and product of apparent density and effective thermal conductivity, ρk_{eff}, vs. the number of radiation shields per unit thickness, *N/t*. 231

Figure 6-73: Compressive mechanical load, *P*, on the multilayer insulation vs. the number of radiation shields per unit thickness, *N/t*. 232

Figure 6-74: Effective thermal conductivity, k_{eff}, and product of apparent density and effective thermal conductivity, ρk_{eff}, vs. the number of radiation shields per unit thickness, *N/t*. 234

Figure 6-75: Effective thermal conductivity, k_{eff}, and product of apparent density and effective thermal conductivity, ρk_{eff}, vs. the number of radiation shields per unit thickness, *N/t*. Complete loading-unloading history of system (△). 235

Figure 6-76: Compressive mechanical load, *P*, on the multilayer insulation vs. the number of radiation shields per unit thickness, *N/t*. 236

Figure 6-77: Compressive mechanical load, *P*, on the multilayer insulation vs. the number of radiation shields per unit thickness, *N/t*. Complete loading-unloading history of system (△). 236

Figure 6-78: Effective thermal conductivity, k_{eff}, and product of apparent density and effective thermal conductivity, ρk_{eff}, vs. the number of radiation shields per unit thickness, *N/t*. 239

Figure 6-79: Effective thermal conductivity, k_{eff}, as a function of the characteristic temperature, *T*. 240

Documents
Document Sharing Hub

Full document details: PD CEN/CLC/TR 17603-31-07:2021

Figure 6-80: Effective thermal conductivity, k_{eff}, and product of apparent density and effective thermal conductivity, ρk_{eff}, vs. the number of radiation shields per unit thickness, *N/t*. 243

Figure 6-81: Effective thermal conductivity, k_{eff}, as a function of the characteristic temperature, *T*. 244

Figure 6-82: Effective thermal conductivity, k_{eff}, and product of apparent density and effective thermal conductivity, ρk_{eff}, vs. the number of radiation shields per unit thickness, *N/t*. 245

Figure 6-83: Compressive mechanical load, *P*, on the multilayer insulation vs. the number of radiation shields per unit thickness, *N/t*. 246

Figure 6-84: Effective thermal conductivity, k_{eff}, and product of apparent density and effective thermal conductivity, ρk_{eff}, vs. the number of radiation shields per unit thickness, *N/t*. 247

Figure 6-85: Compressive mechanical load, *P*, on the multilayer insulation vs. the number of radiation shields per unit thickness, *N/t*. 248

Figure 6-86: Effective thermal conductivity, k_{eff}, and product of apparent density and effective thermal conductivity, ρk_{eff}, vs. the number of radiation shields per unit thickness, *N/t*. 249

Figure 6-87: Compressive mechanical load, P, on the multilayer insulation vs. the number of radiation shields per unit thickness, *N/t*. 250

Figure 6-88: Effective thermal conductivity, k_{eff}, as a function of the characteristic temperature, *T*. 250

Figure 6-89: Lateral effective thermal conductivity, k_{eff}, as a function of characteristic temperature, *T*. 252

Figure 6-90: Lateral effective thermal conductivity, k_{eff}, as a function of characteristic temperature, *T*. 253

Figure 6-91: Lateral effective thermal conductivity, k_{eff}, as a function of characteristic temperature, *T*. 255

Figure 6-92: Lateral effective thermal conductivity, k_{eff}, as a function of characteristic temperature, *T*. 256

Figure 6-93: Effective emittance, $\Delta\varepsilon_{eff}$, vs. overlap, *l* 267

Figure 6-94: Length, *L**, vs. overlap, *l*, of alternate layers. 267

Figure 6-95: Length, *L**, vs. underlap, *l*. 268

Figure 6-96: Length, *L**, vs. k_{eff}. Edge rejection 268

Figure 6-97: Heat loss, ΔQ, due to stitching vs. the length of Stitch, *L*. 270

Figure 6-98: Heat loss, ΔQ, due to stitch patching vs. the number of patch layers, *N*. Undisturbed system and test method as in Figure 6-97. 271

Figure 6-99: Effect of perforations on the effective thermal conductivity of a multilayer insulation formed by 24 Radiation Shields 6,35x10^{-6} m thick Mylar Double-Aluminized, and 23 Spacers 7,11x10^{-4} m thick Polyurethane Foam. 272

Figure 6-100: Effect of perforations on the effective thermal conductivity of a multilayer insulation formed by 10 Radiation Shields 6,35x10^{-6} m thick by 0,279 m diameter Mylar Double-Aluminized, and 22 Spacers 2,54x10^{-5} m thick by 0,305 m diameter Glass Fabric. 273

Documents
Document Sharing Hub

Full document details: PD CEN/CLC/TR 17603-31-07:2021

Figure 6-101: Effect of percentage of perforations, τ, on the heat flux through a multilayer insulation. 274

Figure 6-102: Effect of Meteoroid-Bumper debris damage on the effective thermal conductivity, k_{eff}, and product of apparent density and effective thermal conductivity, ρk_{eff}. 276

Figure 6-103: Effective thermal conductivity, k_{eff}, as a function of gas pressure, p. 278

Figure 6-104: Effective thermal conductivity, k_{eff}, as a function of gas pressure, p. 280

Figure 6-105: Effective thermal conductivity, k_{eff}, as a function of gas pressure, p. 281

Figure 6-106: Effective thermal conductivity, k_{eff}, as a function of gas pressure, p. 283

Figure 6-107: Effective thermal conductivity, k_{eff}, as a function of gas pressure, p. 284

Figure 6-108: Permeability, κ, of several multilayer insulation configurations as a function of the layer density, N/t. 287

Figure 6-109: Pressure differential, $p(0,t)-p_o(t)$. Vs. time, t. 290

Figure 6-110: Knudsen Diffusion Coefficient, D_K, as a function of gas molecular mass, M. From Coston (1967) [13], p. 4,3-31. 292

Figure 6-111: Outgassing rate, Q, as a function of pumping time, t, for Mylar Double-Aluminized. Effect of preconditioning. From Glassford (1970) [24]. 293

Figure 6-112: Outgassing rate, Q, as a function of pumping time, t, for Mylar Double-Aluminized. Effect of prepumping. From Glassford (1970) [24]. 294

Figure 6-113: Outgassing rate, Q, as a function of pumping time, t, for Mylar Double-Aluminized, as received. Effect of test temperature. 295

Figure 6-114: Outgassing rate, Q, as a function of pumping time, t, for several shielding materials, as received. 297

Figure 6-115: Outgassing rate, Q, as a function of pumping time, t, for several spacing materials. 298

Figure 6-116: Outgassing rate, Q, as a function of pumping time, t, for an MLI system and for its components. No preconditioning. From Glassford (1970) [24]. 299

Figure 6-117: Main characteristics of the different self-evacuated MLIs and experimental methods used to obtain the results summarized in Table 6-25. 303

Figure 6-118: Model for a guarded two-dimensional MLI. (a) Geometry. (b) Boundary conditions for the calculations. 317

Figure 6-119: Ratio of lateral to total heat transfer rate, $Q_x/(Q_x+Q_y)$, in an anisotropic two-dimensional continuous medium subject to the boundary conditions indicated in Figure 6-118: 318

Tables

Table 4-1: Relevant Properties of Ceramic Foams 25

Table 4-2: Properties of Ceramic Foams 29

Table 4-3: Characterization of Foams Whose Properties Will Be Given Later 38

Table 4-4: Average Tensile Data of Polyurethane and Polystyrene Foams 39

Table 4-5: Average Tensile Data of Polyurethane and Polystyrene Foams at T = 76 K T: Transverse; L: Longitudinal 40

Documents
Document Sharing Hub

Full document details: PD CEN/CLC/TR 17603-31-07:2021

Table 4-6: Average Tensile Data of Polyurethane and Polystyrene Foams at T = 195 K T: Transverse; L: Longitudinal 41
Table 4-7: Average Tensile Data of Polyurethane and Polystyrene Foams at T = 300 KT: Transverse; L: Longitudinal 42
Table 4-8: Average Compressive Data of Polyurethane and Polystyrene Foams 42
Table 4-9: Average Compressive Data of Polyurethane and Polystyrene Foams at T = 76 K T: Transverse; L: Longitudinal 43
Table 4-10: Average Compressive Data of Polyurethane and Polystyrene Foams at T = 195 K T: Transverse; L: Longitudinal 44
Table 4-11: Average Compressive Data of Polyurethane and Polystyrene Foams at T = 300 K T: Transverse; L: Longitudinal 45
Table 4-12: Information Concerning Processing 60
Table 4-13: Information Concerning Processing of Fiberfil Products Recommendations for Molding 63
Table 5-1: Available Densities, ρ, and Thicknesses, t, of B & W Kaowool Blanket. X denotes available. 90
Table 5-2: Available Thicknesses, t, and Lengths, L, of Fiberfrax Lo-Con Blanket and Felt for densities of64 kg.m^{-3} and 96 kg.m^{-3} and roll widths 0,3 m, 0,61 m, and 1,22 m. 91
Table 5-3: Thermal Conductivity, k, [W.m^{-1}.K^{-1}], of J-M Thermoflex Felt for different values of Density, ρ, [kg.m^{-3}], and Mean Temperature, T_m, [K]. 92
Table 5-4: Available Densities, ρ, [kg.m^{-3}], and Thicknesses, tx10^3 [m], of J-M Thermoflex. 95
Table 5-5: Available Densities, ρ, and Thicknesses, t, of J-M Micro-Quartz 96
Table 5-6: Available Forms of J-M Min-K 1301 102
Table 5-7: Available Forms of J-M Min-K 2000 102
Table 5-8: Available Thicknesses of B&W Kaowool Paper 104
Table 5-9: Available Thicknesses of Fiberfrax 970 Paper 105
Table 5-10: Available Roll Sizes of Fiberfrax 970 Paper 105
Table 5-11: Available Thicknesses and Corresponding Mass/Area of Fiberfrax Paper H880; Hi-Fi 660, and 550. 105
Table 6-1: Properties of Metallic Foils 166
Table 6-2: Properties of Polymeric Films 168
Table 6-3: Properties of Several Marketed Polycarbonate Resins 169
Table 6-4: Tensile Strength of Mylar and Kapton H for Different. Values of the Temperature. 170
Table 6-5: Properties of Coated Plastic Films 170
Table 6-6: Flammability of Several Radiation Shields in Oxygen and in Air 174
Table 6-7: Outgassing Characteristics of Non-Metallized and Metallized Plastic Films 175
Table 6-8: Procurement Data 177
Table 6-9: ρ and 3$\lambda\rho$/8 for Aluminium, Copper, Gold and Silver 182

Documents
Document Sharing Hub
Full document details: PD CEN/CLC/TR 17603-31-07:2021

Table 6-10: Absorption and Scattering Coefficients for Spacer Materials 188
Table 6-11: Properties of Staple Fibers Data is available for the following Staple Fibers 190
Table 6-12: Properties of Staple Fibers 191
Table 6-13: Properties of Staple Fibers 192
Table 6-14: Effect of Heat on Several Fibers 193
Table 6-15: Moisture Regain of Several Fibers 193
Table 6-16: Effect of Exposure Temperature, Pressure and Time on the Strength of Fabrics, *T* = 450 K 194
Table 6-17: Fiber Strength after 10 min Exposure to Temperature 195
Table 6-18: Effect of Cycling vs. Continuous Exposure to Temperature of Two Fibers in Woven Forms 196
Table 6-19: Thermal Properties of Fabrics Woven of Several Fibers 197
Table 6-20: Flammability per Vertical Flame Tests 206
Table 6-21: Flammability of Several Spacers in Oxygen and in Air 206
Table 6-22: Outgassing Characteristics of Several Spacers 207
Table 6-23: Thermal Effects of Joints 259
Table 6-24: Characteristics of Self-Pumping MLIs the performances of which are given in Table 6-25 302
Table 6-25: Characteristics of Several Self-Pumping Multilayer Insulations 304
Table 6-26: Summary of the Best and Worst Cases Reached by the Different Investigators 314

Documents
Document Sharing Hub

Full document details: PD CEN/CLC/TR 17603-31-07:2021

European Foreword

This document (CEN/CLC/TR 17603-31-07:2021) has been prepared by Technical Committee CEN/CLC/JTC 5 “Space”, the secretariat of which is held by DIN.

It is highlighted that this technical report does not contain any requirement but only collection of data or descriptions and guidelines about how to organize and perform the work in support of EN 16603-31.

This Technical report (TR 17603-31-07:2021) originates from ECSS-E-HB-31-01 Part 7A.

Attention is drawn to the possibility that some of the elements of this document may be the subject of patent rights. CEN [and/or CENELEC] shall not be held responsible for identifying any or all such patent rights.

This document has been prepared under a mandate given to CEN by the European Commission and the European Free Trade Association.

This document has been developed to cover specifically space systems and has therefore precedence over any TR covering the same scope but with a wider domain of applicability (e.g.: aerospace).

Documents
Document Sharing Hub

Full document details: PD CEN/CLC/TR 17603-31-07:2021

1 Scope

There are 3 main categories of insulators used in spacecrafts:

1. foams: organic and inorganic;
2. fibrous insulations: for internal and external insulation and for high temperature environments
3. multilayer insulations (MLI): layers of radiation reflecting shields.

Properties, thermal behaviour and application areas of the insulation materials used in spacecrafts are detailed in this Part 7.

The Thermal design handbook is published in 16 Parts

TR 17603-31-01	Thermal design handbook – Part 1: View factors
TR 17603-31-02	Thermal design handbook – Part 2: Holes, Grooves and Cavities
TR 17603-31-03	Thermal design handbook – Part 3: Spacecraft Surface Temperature
TR 17603-31-04	Thermal design handbook – Part 4: Conductive Heat Transfer
TR 17603-31-05	Thermal design handbook – Part 5: Structural Materials: Metallic and Composite
TR 17603-31-06	Thermal design handbook – Part 6: Thermal Control Surfaces
TR 17603-31-07	Thermal design handbook – Part 7: Insulations
TR 17603-31-08	Thermal design handbook – Part 8: Heat Pipes
TR 17603-31-09	Thermal design handbook – Part 9: Radiators
TR 17603-31-10	Thermal design handbook – Part 10: Phase – Change Capacitors
TR 17603-31-11	Thermal design handbook – Part 11: Electrical Heating
TR 17603-31-12	Thermal design handbook – Part 12: Louvers
TR 17603-31-13	Thermal design handbook – Part 13: Fluid Loops
TR 17603-31-14	Thermal design handbook – Part 14: Cryogenic Cooling
TR 17603-31-15	Thermal design handbook – Part 15: Existing Satellites
TR 17603-31-16	Thermal design handbook – Part 16: Thermal Protection System

Documents
Document Sharing Hub
Full document details: PD CEN/CLC/TR 17603-31-07:2021

2 References

EN Reference	Reference in text	Title
EN 16601-00-01	ECSS-S-ST-00-01	ECSS System - Glossary of terms

All other references made to publications in this Part are listed, alphabetically, in the **Bibliography**.

Documents
Document Sharing Hub

Full document details: PD CEN/CLC/TR 17603-31-07:2021

3 Terms, definitions and symbols

3.1 Terms and definitions

For the purpose of this Standard, the terms and definitions given in ECSS-S-ST-00-01 apply.

3.2 Abbreviated terms

The following abbreviated terms are defined and used within this Standard.

F	flammable
NF	non-flammable
LS	linear shrinkage, percent
MLI	multilayer insulation
SE	self-extinguishing
TWL	total weight loss, percent
VCM	volatile condensable materials, percent by weight
gpd	grams per denier

3.3 Symbols

A	area, [m]
C	coefficient for the degradation due to a joint, [m]
D	dissipation factor
$\mathbf{D_K}$	knudsen diffusion coefficient, [$m.s^{-1}$]
E	modulus of elasticity, [Pa]
$\mathbf{E_c}$	compressive modulus of elasticity, [Pa]
$\mathbf{E_f}$	flexural modulus of elasticity, [Pa]

Documents
Document Sharing Hub

Full document details: PD CEN/CLC/TR 17603-31-07:2021

F	propagating tear strength in a foil, [N]
F_{HC}	View factor, fraction of the total radiation which arrives at *C* coming from *H*
K_0	constant dependent on the interaction between gas and porous medium, [m]
L	length, [m]
L*	equivalent length for the degradation because of a joint, [m]
M	gas molecular mass, [$kg.mol^{-1}$]
N	Clause 5: factor relating the radiative contribution to the effective thermal conductivity of a foam to the warm boundary temperature Clause 7: number of shields in an MLI, number of patch layers in an MLI
N_A	Avogadro constant, N_A = 6,02252x10^{23} mol^{-1}
P	applied compressive load, [Pa]
Q	heat flow through the insulation, [W] outgassing rate, [$Pa.m.s^{-1}$]
R	electrical resistance of a foil, [Ω per Square] boltzmann constant, *R* = 1,38054x10^{-23} $J.K^{-1}$
R(2π,β')	reflectance factor, irradiation over a complete hemisphere
S	steric factor accounting for the distortion of the heat flow path due to foam expansion
T	temperature, [K]
T_m	arithmetic mean temperature, [K]
V	gas volume flow rate per unit area of the insulation, [$m.s^{-1}$]
a	absorption coefficient, [m^{-1}]
c	specific heat, [$J.kg^{-1}.K^{-1}$]
c_p	gas specific heat at constant pressure, [$J.kg^{-1}.K^{-1}$]
$\bar{c}$	average molecular speed, [$m.s^{-1}$], $\bar{c} = (8RT/\pi m)^{1/2}$
d	diameter, [m]

Documents
Document Sharing Hub
Full document details: PD CEN/CLC/TR 17603-31-07:2021

f	frequency, [Hz]
h	thermal conductance, [$W.m^{-2}.K^{-1}$]
k	thermal conductivity, [$W.m^{-1}.K^{-1}$]
$\mathbf{k_g}$	gas thermal conductivity, [$W.m^{-1}.K^{-1}$]
$\mathbf{k_{rad}}$	radiative contribution to the effective thermal conductivity, [$W.m^{-1}.K^{-1}$]
m	mass of one molecule, [kg]
m	mass flow rate per unit cross-sectional area, [$kg.m^{-2}.s$]
$\mathbf{m_h}$,	mass flow rate per unit cross-sectional area of an isolated hole, [$kg.m^{-2}.s$]
n,	refractive index
$\mathbf{n_s}$	number of space layers per shield
p	gas pressure, [Pa]
	Clause 7: fraction of the electrons suffering specular reflection at the surface of a metallic film
$\mathbf{p_o}$	ambient pressure, [Pa]
s	scattering coefficient, [m^{-1}]
t	insulation thickness, [m]
t'	spacer thickness, [m]
$\mathbf{t_c}$	coating thickness, [m]
$\mathbf{t_{c\Omega}}$	coating thickness as measured by the electrical resistance method, [m]
$\mathbf{t_u}$	uncompressed insulation thickness, [m]
t	time, [s] or [min]
w	width, [m]
x	geometrical coordinate
ΔL/L	linear thermal expansion
α	Clause 6: sound absorption coefficient.
	Clause 7: absorptance, thermal diffusivity
α_s	normal solar absorptance

Documents
Document Sharing Hub
Full document details: PD CEN/CLC/TR 17603-31-07:2021

α'_λ	directional spectral absorptance
β	Clauses 5 and 7: linear thermal expansion coefficient
	Clause 7: angle between surface normal and direction of incident flux, [angular degrees]
β'	angle between surface normal and direction of reflected, emitted or transmitted flux, [angular degrees]
δ	strain
ε	hemispherical total emittance
ε_a	apparent emittance of a groove
ε_r	dielectric constant
ε'	directional total emittance
θ	groove angle, [angular degrees]
κ	permeability of a porous medium, [m^2]
λ	wavelength of the incident radiation, [m]
	mean free path, [m]
μ	dynamic viscosity, [Pa.s]
π	pressure differential, [Pa]
ρ	density, [$kg.m^{-3}$]
	Clauses 5 and 7: reflectance
	Clause 7: bulk electrical resistivity, [Ω.m]
σ	Clauses 5 and 7: Stefen-Boltzmann constant, σ= 5,6697x10^{-8} $W.m^{-2}.K^{-4}$
	Clause 5: strength, either tensile, compressive or flexural, [Pa]
σ_0	yield strength, [Pa]
τ	Clause 5: shear strength, [Pa]
	Clause 7: fractional area of perforations or transmittance of a perforated shield
τ_0	shear yield strength, [Pa]

Documents
Document Sharing Hub

Full document details: PD CEN/CLC/TR 17603-31-07:2021

Subscripts

C	cold boundary
H	hor boundary
e	concerns MLI evacuation by edge-controlled pumping
eff	effective
eff(nor)	normal effective ((nor) is omitted except when normal and lateral heat transfer appear simultaneously)
eff(lat)	lateral effective (same comment as for (nor))
h	concerns MLI evacuation by hole-controlled pumping
i	concerns the ith Layer or the ith joint of an MLI
ult	concerns ultimate strength

Superscripts

j	concerns species *j*

Documents
Document Sharing Hub
Full document details: PD CEN/CLC/TR 17603-31-07:2021

4 Foams

4.1 General

Foams are commonly used as insulating materials in building, storage vessels, sports equipment, spacecraft, and others. They can be also used for potting and encapsulation of shock-sensitive components and for packaging. Because they have many advantages for cryogenic and space applications, efforts have been made to develop suitable foams; establish their physical, chemical and structural properties, and integrate foams with thermal insulation systems.

Because of their cellular structure of discrete or interconnected voids, a large percentage of the foam volume is air, or whatever gas used as the expanding agent, thence foams are light-weight and very low thermal conductivity, that could be decreased further by evacuation. In most cryogenic applications the insulation efficiency is achieved by condensation of the gases contained in the cellular structure of the plastic material (cryopumping).

The main shortcomings of the foams are that they are not gas-tight, that their mechanical properties are relatively poor, and that thermal stresses induce cracks which require the use of constrictive wraps to maintain the insulation integrity.

According to their chemical composition foams may be classified in inorganic and organic.

Inorganic foams have been used at elevated temperatures. These foams are difficult to produce and have inferior physical properties than organic foams at low densities (16 to 80 $kg.m^{-3}$).

Organic foams, on the other hand, can be readily manufactured in low densities. These foams are used, in the range of cryogenic temperatures, either as a single insulation or combined with other materials to form an integrated system.

Three basic problems should be considered regarding the application of organic foams as thermal insulators, namely: thermal conductivity, thermal expansion and contraction, and flammability and explosion hazards.

1. Thermal Conductivity. Thermal conduction through a foam combines solid conduction, gas conduction and radiation. Although an effective thermal conductivity, in the Fourier law sense, can be measured with relative ease, analytical models are available for predicting the thermal conductivity and the net heat flow through candidate foam materials to be used as thermal insulators.

The solid thermal conductivity of most foams varies with temperature in an almost linear manner as with many other materials. When the density decreases, the solid conductivity will be reduced, not only because the decreasing of the solid cross section, but also by the influence of a steric factor since, even assuming that the shape of the cells is independent of the density, expansion elongates the paths through which heat flow. As an illustration Figure 4-1 shows the calculated variation of the thermal conductivity of a polyurethane resin as a function of foam density.

Documents
Document Sharing Hub

Full document details: PD CEN/CLC/TR 17603-31-07:2021

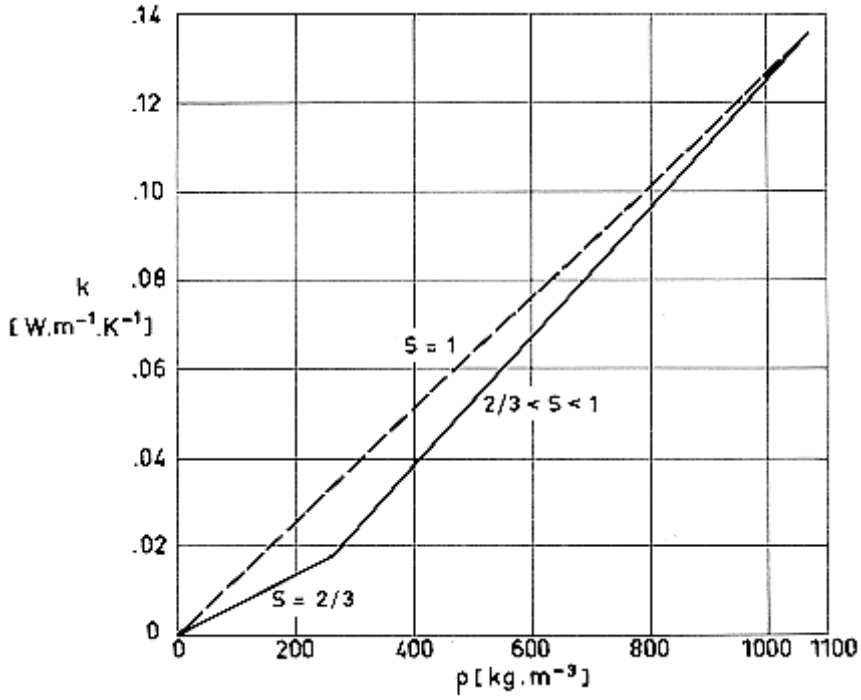

Note: non-si units are used in this figure

Figure 4-1: Resin thermal conductivity

k, as a function of foamed resin density, *ρ*. *S* is the steric factor which takes into account the distortion of the heat flow paths because expansion of the foam. Polyurethane resin. From Hammond (1969) [28].

The second mode of heat transfer of heat is heat conduction. In the case of closed-cell foams the gas thermal conductivity is a function of the concentration of both the foaming agent and the air which may diffuse into the foam outside. Since condensation can take place the thermal conductivities of both gases will depend not only on temperature but also on pressure. Figure 4-2 gives the gas thermal conductivity for mixtures of Freon 11, a typical foaming agent, and air, at atmospheric pressure, as function of temperature.

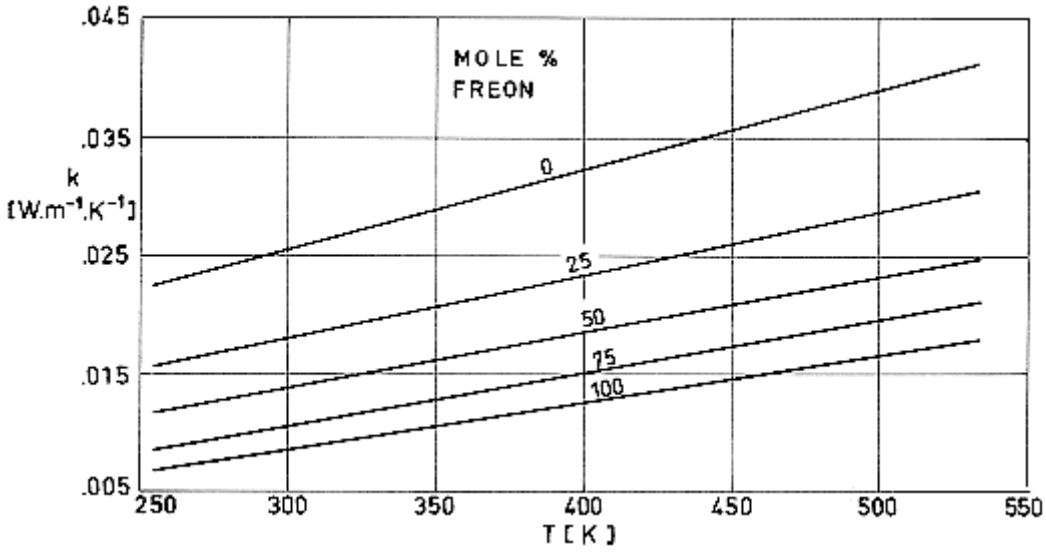

Note: non-si units are used in this figure

Figure 4-2 : Gas thermal conductivity

Documents
Document Sharing Hub
Full document details: PD CEN/CLC/TR 17603-31-07:2021

k, for mixtures of Freon 11 and air as a function of temperature, T, for different concentrations of Freon 11. From Hammond (1969) [28].

In most spacecraft applications the foam is outgassed, so that the gas conductivity is kept small enough to be neglected as compared with the other thermal conductivities. However, in the case of foams sprayed on cryogenic tanks for insulating purposes, the air has enough time to diffuse into the foam, possibly degrading the insulation characteristics in an amount which can be estimated. For example: in a typical case (Schroeder (1973)b [61]) a total cure of 72 hours is required, after spraying the foam, before the cryogenic exposure of the tank wall.

The radiative transfer of heat within the foam involves simultaneous transmission, absorption and scattering. According to Hammond (1969) [28] the radiative contribution to thermal conductivity of the foam can be written as

$$k_{rad} = N\sigma \frac{T_H^4 - T_C^4}{a\left(T_H - T_C\right)} = 4N\sigma \frac{T_H^3}{a} \qquad [4\text{-}1]$$

where: N is a constant factor which lies between 0,5 (for low temperatures) and 2 (for high temperatures).
T_C, T_H are the cold and warm boundary temperatures, respectively. [K].

a is the foam absorption coefficient. [m^{-1}].

σ is the Stefan-Boltzmann Constant. [$W.m^{-2}.K^{-4}$].

Values of the radiation thermal conductivity are given in Figure 4-3 versus mean temperature, T_m. It can be deduced from this figure that radiation becomes significant above 350 K.

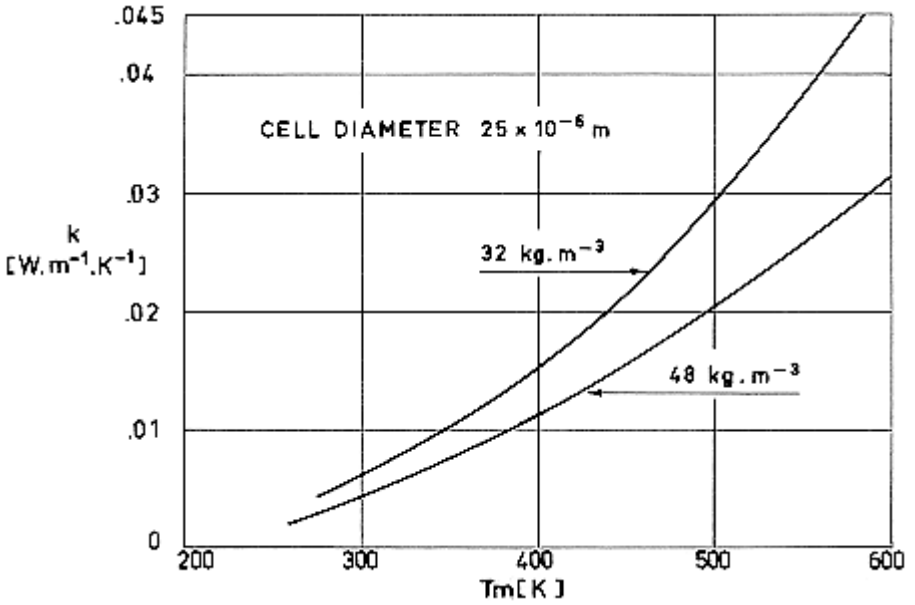

Figure 4-3: Radiation thermal conductivity

k_{rad}, as a function of mean temperature, T_m, for two polyurethane foams. From Hammond (1969) [28].

2. Thermal Expansion and Contraction. Broadly speaking, the thermal expansion coefficient of polyurethane foams is 2 to 5 times that of aluminium and 4 to 10 times that of steel. Because of this large difference in thermal expansions, the foam cannot be foamed in place against the metal or

Documents
Document Sharing Hub
Full document details: PD CEN/CLC/TR 17603-31-07:2021

bonded directly to it, since during chilldown from ambient temperature to cryogenic temperatures high stresses are created in the foam, and it fail either in shear along the tank surface or in tension in direction normal to it.

Various techniques for overcoming the effects of thermal contraction have been developed. For example, Glaser et al. (1967) [23], report that the addition of 10 percent (based on the weight of foam) of chopped glass fibers, $6{,}35 \times 10^{-3}$ to $12{,}7 \times 10^{-3}$ m long, to a low-viscosity one-shot foam eliminated cracking of the foam when exposed to liquid nitrogen. The same authors indicate that in work on the Saturn S-IV stage, where an internal insulation system was developed for the liquid-hydrogen propellant tank, urethane foam was reinforced with threads in order to prevent foam failure.

3. Fire and Explosion Hazards. The fire hazard of plastic materials has been demonstrated in the most dramatic fashion many times. Depending upon anticipated use, some polymeric materials are required to pass various flammability tests. The passing of these tests is assured by the addition of fire retardants.

When external foam insulation is used in spacecraft tankage, the possibility of ignition can be enhanced by the diffusion of air into foam. Because of the low temperatures the air condenses, and this oxygen rich condensed air, in conjunction with an oxidizable organic foam, can create an explosion hazard.

Flame-retardant coatings can be applied to the exterior of the insulation, once it has been cured, to enhanced its self-extinguishing characteristics. When this precaution has been taken, the possibility of ignition or explosion in a well-designed foam insulation system is remote.

A further hazard associated with burning of foams is the toxicity of their combustion products, which can be ascribed to the fire-retardant additives. Petajan et al. (1975) [51] report that the physiological and toxicological effects of the combustion products of a laboratory-formulated fire-retarded rigid-polyurethane foam, proved fatal to rats in a matter of minutes, while the same rigid-polyurethane foam, without fire retardant, produced only minor signs of toxicity. The fire-retardant used in these experiments, a reactive phosphate, is not uncommon in the commercial formulations.

4.2 Inorganic foams

Porous ceramic foams have been developed to be used as high temperatures insulators, for space applications. These foams provide the high strength required in many instances. Nevertheless, their use is somewhat limited because of their high density and relatively high thermal conductivity.

Table 4-1 gives the relevant properties of several ceramics foams.

The influence of temperature on thermal conductivity and linear thermal expansion of the same types of foam is shown in Figure 4-4 and Figure 4-5 respectively.

Table 4-1: Relevant Properties of Ceramic Foams

	Alumina	Silica	Silicon Carbide	Zircon
Maximum Recommended Service Temperature [K]	2090	1920	2200	2470
Porosity [percent]	88	84	90	86
Density, $\rho x10^{-3}$ [kg.m^{-3}]	0,51	0,32	0,32	0,74

Documents Document Sharing Hub

Full document details: PD CEN/CLC/TR 17603-31-07:2021

Thermal Conductivity, k, [W.m^{-1}.K^{-1}]	0,605	0,158	0,821	0,137
Compressive Strength, σ_{ult}x10^{-6} [Pa]	6,41	5,31	1,38	1,65

NOTE From Glaser et al. (1967) [23].

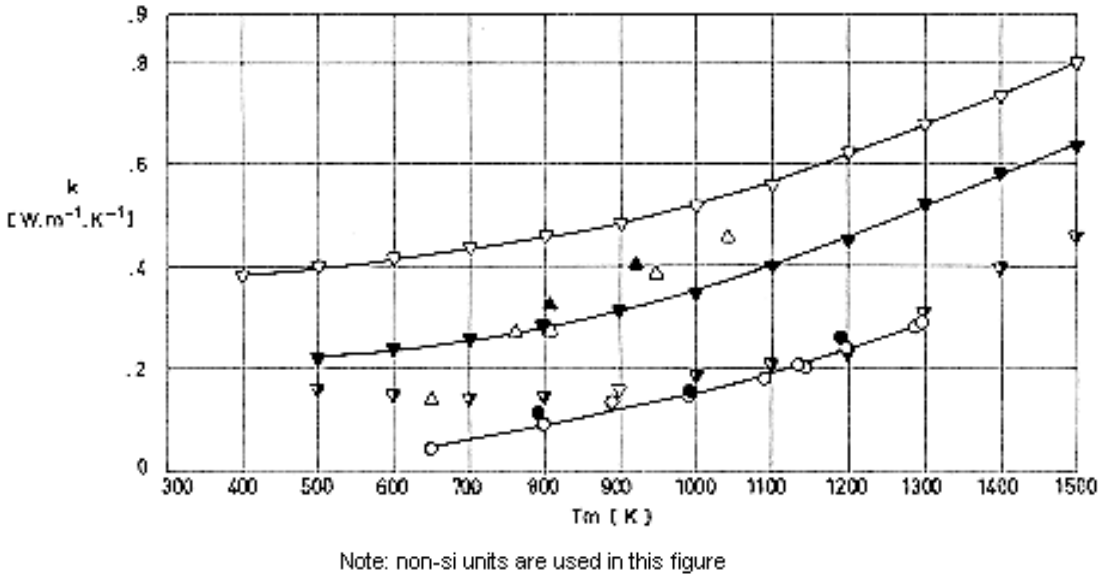

Figure 4-4: Thermal conductivity, k, of several ceramic foams as a function of arithmetic mean temperature, T_m.

Explanation

Key	Description	Comments	References
○	Alumina. Density, ρ = 470 kg.m^{-3}.	Measured in 5,33x10^{-5} to 2,66x10^{-2} Pa pressure range.	Touloukian (1967)a [72].
●	Same as above.	Measured when cooled.	
△	Silicon Carbide. Density, ρ = 460 kg.m^{-3}.	Measured in 5,33x10^{-5} to 4x10^{-2} Pa pressure range.	Touloukian (1967)b [73].
▲	Same as above.	Measured when cooled.	
▽	Zircon. Density, ρ = 960 kg.m^{-3}.	Data extracted from smooth curve.	Glaser et al. (1967) [23].
▼	Zircon Z-90. Density, ρ = 940 kg.m^{-3}.		

Documents
Document Sharing Hub
Full document details: PD CEN/CLC/TR 17603-31-07:2021

▽	Zircon Z-67. Density, $\rho = 830$ kg.m^{-3}.		

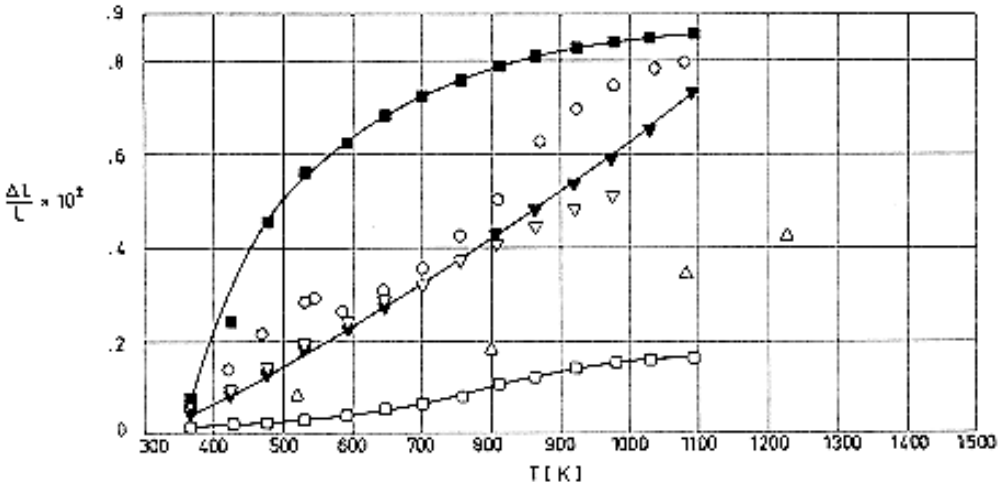

Note: non-si units are used in this figure

Figure 4-5: Linear thermal expansion, $\Delta L/L$, of several ceramic foams as a function of temperature, T.

Explanation

Key	Description	Comments	References
○	Alumina. 35-40 alumina hidrate, 25-30 Al_2O_3, 22-27 H_3PO_4 (85%), 8-12 H_2O, 1-1,5 carbon powder, and 0,05-0,1 Al powder. Density, $\rho = 930$ kg.m^{-3}. Dimensions, 5,08x10^{-2} m long by 6,35x10^{-3} m square.	Cured at 366 K; temperature raised continuously to 588,5 K during a 20 h period and then held at this temperature for 12 h. Reference temperature not given, assumed to be 293 K.	Touloukian (1967)a [72].
□	Silica. 50-55 Glasrock Slip, 30-35 Ludox (colloidal SiO_2), 5-7 SiO_2 400 mesh, 3-6 Al powder, 3-6 carbon powder, and 2-3 microballons. Density, $\rho = 640$ kg.m^{-3}. Dimensions, 5,08x10^{-2} m long by 6,35x10^{-3} m square.	Cured at 366 K; temperature raised continuously to 588,5 K during a 24 h period and then held at this temperature for 8 h. Reference temperature not given, assumed to be 293 K.	
■	Same as above.	Second run.	
△	Silicon Carbide. Carborundum Company.	Measured in vacuum of 1,7x10^3 Pa up to 1200 K and with a slight	Touloukian (1967)b [73].

Documents
Document Sharing Hub
Full document details: PD CEN/CLC/TR 17603-31-07:2021

	Density, $\rho = 610$ kg.m^{-3}. Dimensions, 7,62x10^{-2} m long by 1,27x10^{-2} m diameter.	purge of argon above 1200 K.	
∇	Zircon. 30-35 ZrO_2 100 mesh, 20-25 ZrO_2 325 mesh, 20-25 of 90 rare-earth oxide, 10-12 H_3PO_4, 10-12 H_2O, 1-2 carbon powder, and 0,05-0,1 Al powder. Density, $\rho = 1600$ kg.m^{-3}. Dimensions, 5,08x10^{-2} m long by 6,35x10^{-3} m square.	Cured at 366 K; temperature raised continuously to 588,5 K during a 20 h period and then held at this temperature for 24 h. Reference temperature not given, assumed to be 293 K.	Touloukian (1967)c[74] .
▼	Same as above.	Second run.	

Zircon foams that can be cast and later cured in place at temperatures below 390 K have been developed. These foams have excellent insulating and structural properties and are suitable for use in rigid heat shields. Figure 4-6 shows the temperature evolution of the hot face, T_H, and back face, T_C, of several pieces of zircon foam which are heated by a heat flux of 4,5x10^5 W.m^{-2}. To perform the tests the foams were placed in contact with a stainless-steel honeycomb panel exposed to the heat flux.

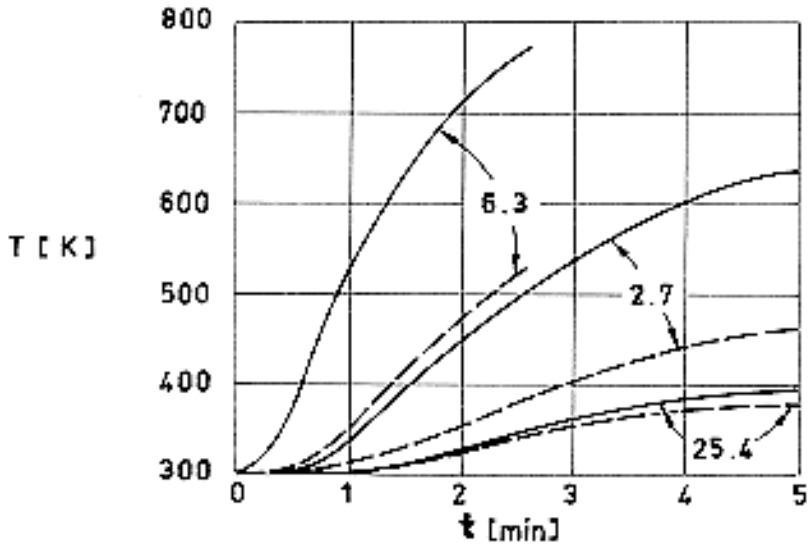

Note: non-si units are used in this figure

Figure 4-6: Temperature evolution of the hot and cold faces of several pieces of Zircon foam. Solid line: T_H, hot face. Dashed line: T_C, cold face.

The numbers in the figure indicate the foam thickness in mm. From Glaser et al (1967) [23].

Impregnated porous ceramics may also be used as insulating materials (Glaser et al, (1967) [23]). These foams consist of a refractory porous base uniformly impregnated with a solid substance which sublimes or decomposes at elevated temperatures. Phenolics, and thermoplastics such as nylon, polyethylene, and polypropylene, have been used as the impregnating material. The composite is very similar to ablative substances used in reentry heat shields; although it presents the advantage that no changes in the shape of the surface occur.

Documents
Document Sharing Hub
Full document details: PD CEN/CLC/TR 17603-31-07:2021

Thermal switches formed by ceramic foams impregnated with metals such as silver or copper can be used to protect radioisotope capsules from reentry heating (Bustard, Princiotta & Barr (1970) [9]). These composites are thermal conductors ($k \cong 9$ W.m^{-1}.K^{-1}) below the melting point of the metal impregnate and switch to insulators ($k \cong 0{,}2$ W.m^{-1}.K^{-1}) above its melting point. In this manner, the thermal conductance during normal power system operation is relatively high, facilitating the transfer of heat from the fuel capsule to the hot side of the energy conversion device, without excessive capsule and/or radioisotope temperatures. During reentry into the earth's atmosphere the capsule is protected against the aero thermodynamic heating by the unimpregnated ceramic foam.

Table 4-2, which has been borrowed from Bustard et al. (1970) [9], gives additional properties of several ceramic foams.

Table 4-2: Properties of Ceramic Foams

Description	Alumina Ipsen 3300	Alumina Ipsen 3400	Alumina Astro Met 200	Alumina Insalute	Fused Silica Glassrock 25
Chemical Formula	Al_2O_3	Al_2O_3	Al_2O_3	Al_2O_3	SiO_2
Thermal Conductivity, k, at 1350 K, [W.m^{-1}.K^{-1}]	0,64	0,52	0,69	0,40	0,28
Specific Heat, cx10^{-3} at 1350 K, [J.kg^{-1}.K^{-1}]	1,34	1,34	1,34	1,34	1,46
Melting Point [K]	2320	2320	2320	2320	2000
Density, ρx10^{-3} [kg.m^{-3}]	0,92	0,56	0,39	0,85	0,42
Pore Structure	Coarse pore-bubble structure	Coarse pore-bubble structure	Open pore-lacey structure	Irregular pore	Fine pore-bubble structure
Thermal Shock Resistance	Good-bairline cracks developed	Fair to poor-spalling	Very poor-severe cracking	Fair to poor-cracking and spalling	Excellent-no structural damage
Compressive Strength, σ_{ult}x10^{-6} [Pa]	6,20	4,83	0,34	2,31	3,10
Shear Strength, τ_{ult}x10^{-6} [Pa]	3,59	3,03	0,69	1,24	1,72

Documents
Document Sharing Hub
Full document details: PD CEN/CLC/TR 17603-31-07:2021

Machinability	Fair	Good	Very poor	Fair	Excellent

Description	Fused Silica Thermo Matls. 50	Fused Silica Thermo Matls. HP50	Zircon Ipsen 4400	Zircon Ipsen 4300
Chemical Formula	SiO_2	SiO_2	ZrO_2 [a]	ZrO_2 [b]
Thermal Conductivity, k, at 1350 K, [$W.m^{-1}.K^{-1}$]	0,38	0,38	0,40	0,40
Specific Heat, $c x10^{-3}$ at 1350 K, [$J.kg^{-1}.K^{-1}$]	1,46	1,46	0,75	0,75
Melting Point [K]	2000	2000	2960	2960
Density, $\rho x10^{-3}$ [$kg.m^{-3}$]	0,80	0,80	1,45	1,10
Pore Structure	Fine pore-bubble structure	Fine pore-bubble structure	Coarse pore-bubble structure	Coarse pore-bubble structure
Thermal Shock Resistance	Excellent-no structural damage	Excellent-no structural damage	Good-no structural damage	Poor-severe cracking
Compressive Strength, $\sigma_{ult} x10^{-6}$ [Pa]	12,1	22,4	6,14	5,51
Shear Strength, $\tau_{ult} x10^{-6}$ [Pa]	3,45	5,38	3,72	3,79
Machinability	Excellent	Excellent	Fair	Good

[a] Partially stabilized to cubic structure.

[b] Fully stabilized to cubic structure.

NOTE From Bustard, Princiotta & Barr (1970) [9].

Documents
Document Sharing Hub

Full document details: PD CEN/CLC/TR 17603-31-07:2021

4.3 Organic foams

Low density organic foams are used for cryogenic insulation because they offer the following advantages:

1. Ease of fabrication,
2. Relatively low cost, and
3. Self-supporting structure.

Like plastics, organic polymer foams can be divided into two basic groups: thermoplastic foams and thermosetting foams.

Thermoplastic foams soften at temperatures of 340 to 390 K and, in most cases, tend to become brittle at cryogenic temperatures. These foams can be made from such polymers as cellulose acetate, polystyrene, styrene-acrylonitrile copolymer, polyvinylchloride, polyethylene, and polypropylene. Among these foams polystyrene and polyvinyl-chloride are the most commonly used. Polystyrene foams are rigid and polyvinyl chloride are flexible, although rigid PVC foams have been developed recently which are competitive with other rigid foams.

Thermosetting foams are commonly made with phenolic, urea-formaldehyde, epoxy, and polyurethane resins. Flexible polyurethane foams dominate the market; these foams exhibit very good properties at cryogenic temperatures with a minimum tendency to become brittle. Urea-formaldehyde foams are brittle and do not show good structural properties at low densities. Low density phenolic resin foams tend to be brittle and friable at room temperature and are difficult to manufacture. Epoxy foams have met only with limited use because of difficulties in controlling satisfactorily the foaming.

Tetrafluoroethylene foam (TFE) is an intermediate material between a thermosetting and a thermoplastic foam. It melts at very high temperature, has very good physical properties at cryogenic temperatures and, because of its extreme chemical inertness, resists the effects of liquid oxygen, hydrazine, and other chemically reactive rocket fuels.

Documents
Document Sharing Hub

Full document details: PD CEN/CLC/TR 17603-31-07:2021

4.3.2 Thermal properties of organic foams

Figure 4-7 summarizes the available information on the thermal conductivity of polyurethane foams in a wide range of temperatures, and for different foam densities and preconditioning. Data for polystyrene foams are given in Figure 4-8.

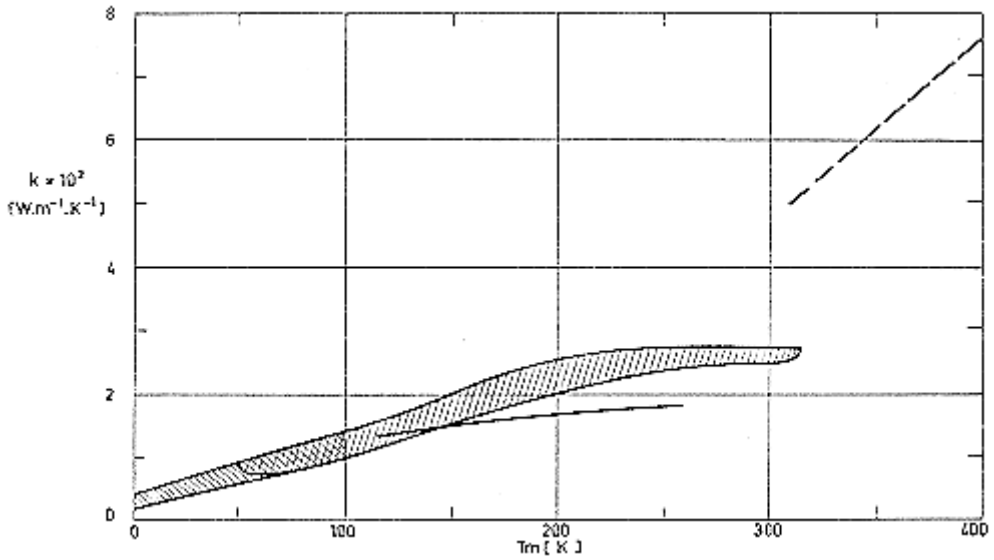

Figure 4-7: Thermal conductivity k, of polyurethane foams vs. arithmetic mean temperature, T_m.

Left-oriented shadowed area: 64 kg.m^{-3} > ρ > 32 kg.m^{-3}; cryopumped; from Coston (1967).
Right-oriented shadowed area: From Rosato (1968) [56].
Solid line: CO_2 blown, ρ = 32 kg.m^{-3}; evacuated; from Schroeder (1973)b [61].
Dashed line: The same foam at ambient pressure in air; from Schroeder (1973)b [61].

Documents
Document Sharing Hub
Full document details: PD CEN/CLC/TR 17603-31-07:2021

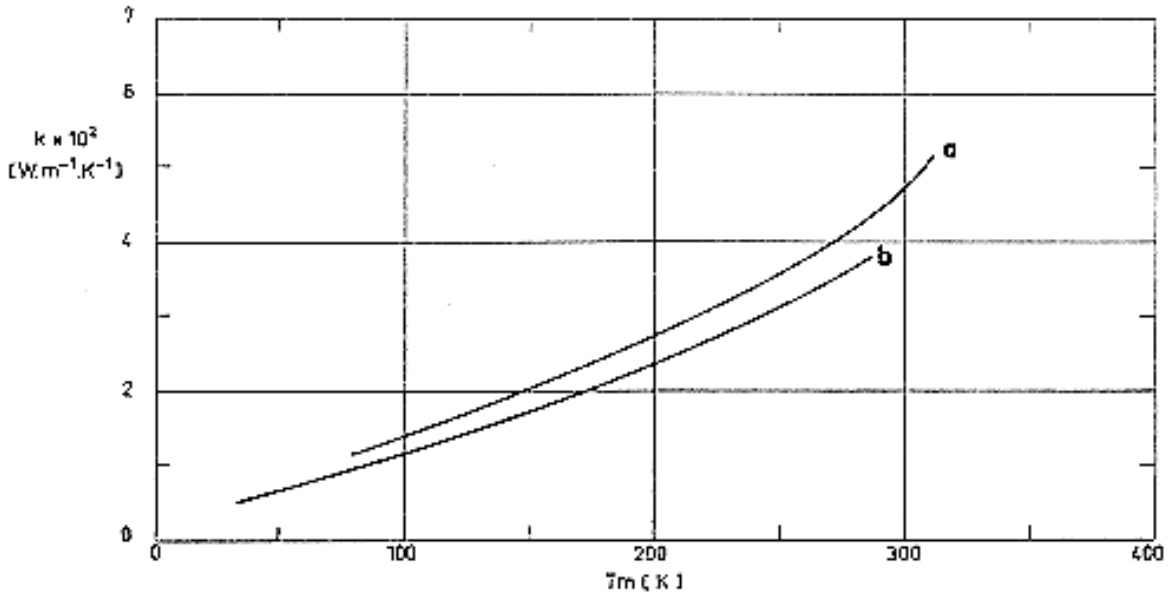

Figure 4-8: Thermal conductivity, *k*, of cryopumped polystyrene foams.

a: Styrofoam, $\rho = 33$ kg.m^{-3}. *b*: Styrofoam, $\rho = 22$ kg.m^{-3}. Styrofoam is a registered trade name of Dow Chemical Co. From Rosato (1968) [56].

As has been already said, the thermal conductivity of foams can be reduced further by evacuation.

Evacuation by vacuum pumps is used when foams are employed as spacers of multilayer insulations. However, for insulating relatively large cryogenic tanks pump evacuation is normally impractical, nevertheless, in that case the gas contained in the cellular structure condenses because of the prevailing low temperature level, thus leaving the void space evacuated (cryopumping).

A close examination of the thermal conductivity-temperature curve in the proximity of the condensation temperature of the filling gas reveals the typical S-curve behavior shown in Figure 4-9. This particular curve corresponds to a Freon 11-air filled foam. At atmospheric pressure Freon 11 condenses between 260 and 290 K. At temperatures below 260 K air controls the gas conduction contribution to the foam thermal conductivity. This contribution decreases when the temperature decreases, reaching very low levels when the air condenses. In the temperature range above the Freon condensing temperature the gas conduction depends on the concentration of Freon in the binary Freon-air system, and on temperature, increasing when the temperature increases, as occurs with single-phase gaseous systems. In the intermediate temperature range, when Freon starts boiling, the conductivity of the gaseous system decreases since the thermal conductivity of Freon is about a fourth of that of air.

Documents
Document Sharing Hub
Full document details: PD CEN/CLC/TR 17603-31-07:2021

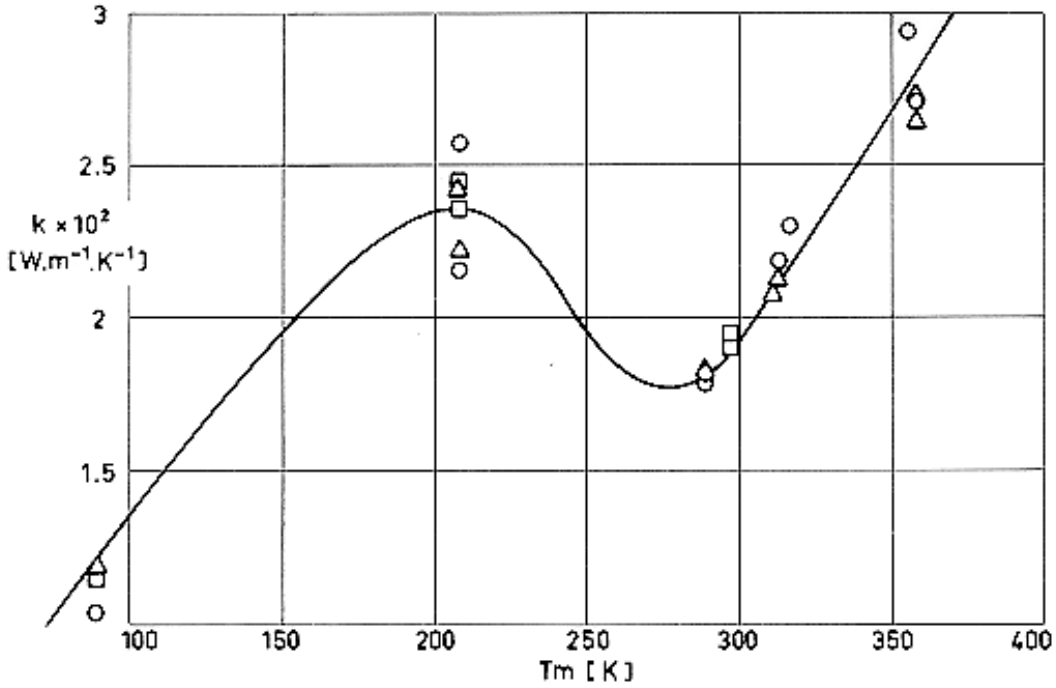

Figure 4-9: Thermal conductivity, k, vs. arithmetic mean temperature, T_m, of a polyurethane foam in the proximity of the condensation temperature of the filling gas.

The temperature gradient is parallel to the foam rise direction. Foam: Nopcofoam BX-250, two-component, flame retardant, spray foam. Filling gas: Freon 11.
○: $\rho = 30{,}6$ kg.m^{-3}.
□: $\rho = 32{,}7$ kg.m^{-3}.
△: $\rho = 37{,}5$ kg.m^{-3}.
From Schroeder (1973)b [61].

Linear thermal expansion of relevant foams is shown in Figure 4-10. It can be seen that Epoxy foams have the lowest thermal expansion. For a given foam, the thermal expansion increases when the temperature increases. Especially significant is the fact that in the cryogenic range all the foams have thermal expansion characteristics which can be reasonably considered as linear functions of temperature, the nonlinearities becoming apparent at room temperature.

Documents
Document Sharing Hub
Full document details: PD CEN/CLC/TR 17603-31-07:2021

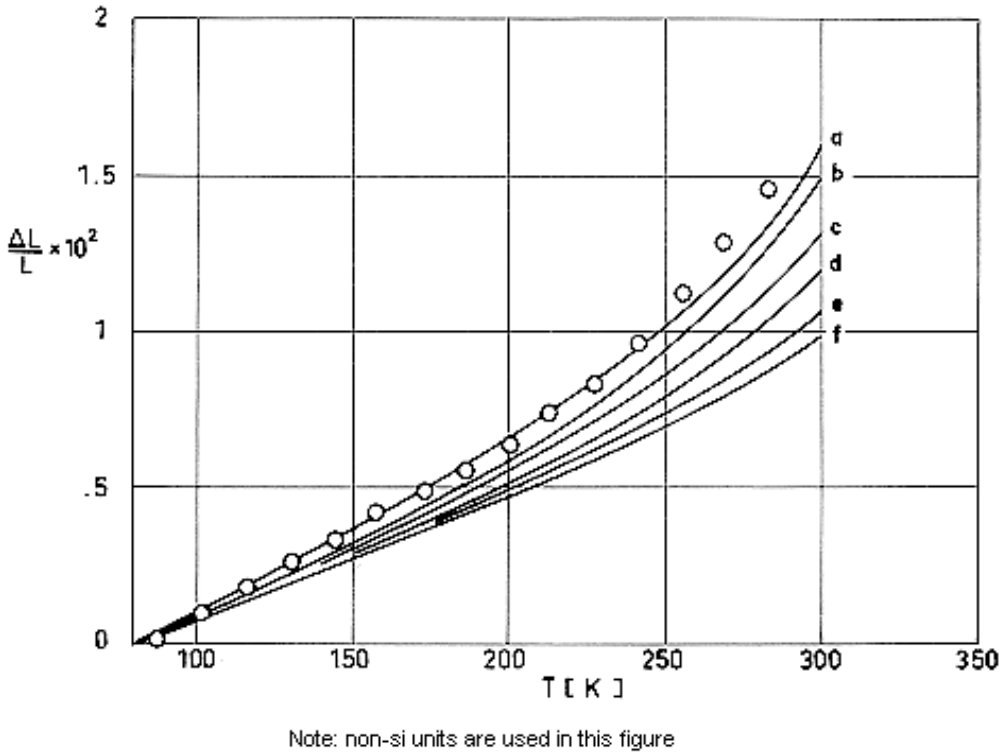

Figure 4-10: Linear thermal expansion, $\Delta L/L$, of several organic foams as a function of temperature, T.

○: Polyurethane foam. $\rho = 50$ kg.m^{-3}. From Schroeder (1973)b [61].
a Urethane foam. $\rho = 80$ kg.m^{-3}.
b Urethane joint filler.
c Syntactic foam. Urethane filler with hollow silica spheres.
d Semiflexible Urethane.
e Epoxy.
f Epoxy.
Curves *a* to *f* are from Glasser et al. (1967) [23].

4.3.3 Mechanical properties of organic foams

In general, the main function of an insulation system is to provide thermal protection; it is not intended to be a primary load-carrying structure. However, since the insulation system is normally bonded or mechanically attached to the primary structure, it should match the strains and deflections of that structure, and therefore significant stresses could be introduced in it.

Low temperature mechanical property data of foams are extremely scarce, notwithstanding the fact that they are required for efficient design of foam-based insulations. Because of these reasons it seems advisable to collect these data in the present item.

The tensile strengths of a number of foams at temperatures ranging from 400 K down to 20 K are shown in Figure 4-11. At 20 K both the semirigid polyurethane and the epoxy foams have tensile strengths of the order of 4x10^5 Pa. At room temperature the rigid polyurethane foam has the highest tensile strength, closely followed by the semirigid polyurethane foam. At room temperatures of the order of 400 K the tensile strength of all the organic foams practically vanishes.

Documents
Document Sharing Hub
Full document details: PD CEN/CLC/TR 17603-31-07:2021

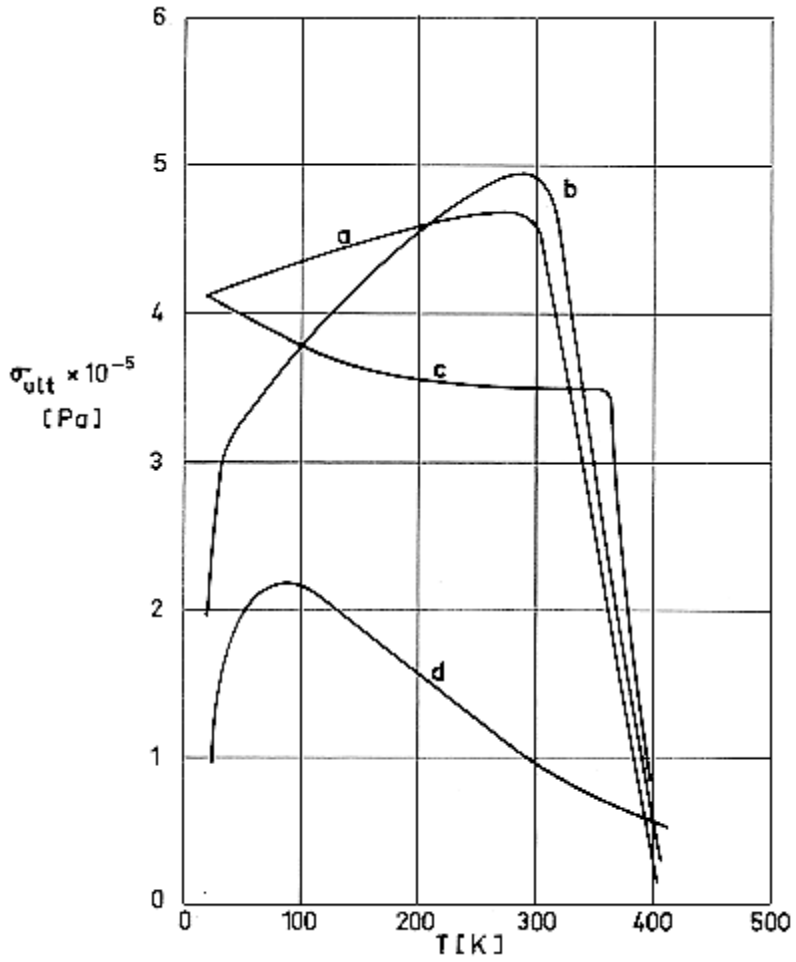

Figure 4-11: Ultimate tensile strength, of several foams as a function of temperature, *T*.

a: Barret semirigid polyurethane.
b: Hexcel 1414-2 polyester polyurethane rigid.
c: Magnolia 7015 epoxy.
d: Baron S-39 flexible polyester.
From Rosato (1968) [56].

The results of shear strength tests are summarized in Figure 4-12. All the foams tested exhibit minimum shear strengths at the two extreme temperatures. Again the rigid polyurethane foam has the highest shear strength among all of them.

Documents
Document Sharing Hub
Full document details: PD CEN/CLC/TR 17603-31-07:2021

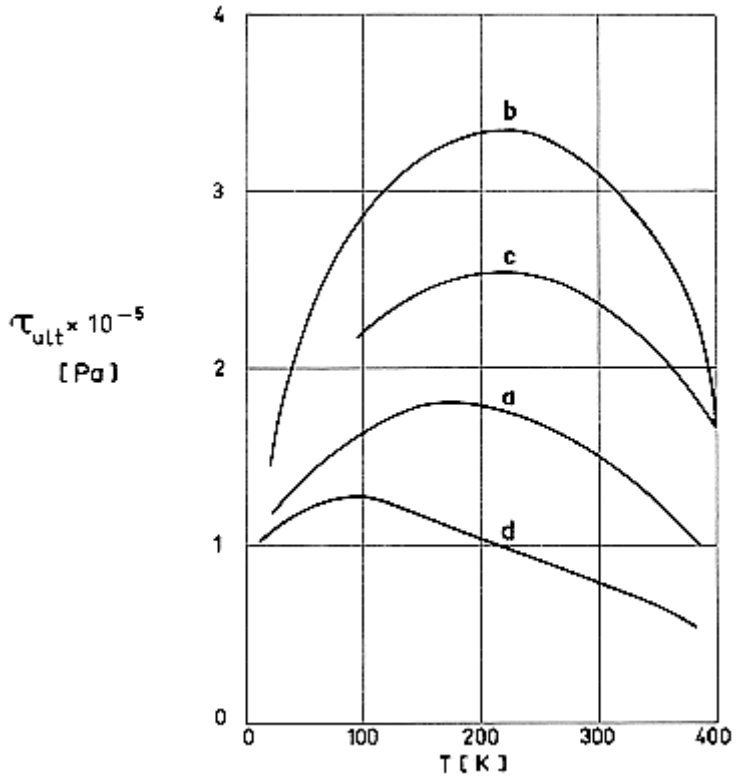

Figure 4-12: Ultimate shear strength, τ_{ult}, of several foams as a function of temperature, T.

a: Barret semirigid polyurethane.
b: Hexcel 1414-2 polyester polyurethane rigid.
c: Magnolia 7015 epoxy.
d: Baron S-39 flexible polyester.
From Rosato (1968) [56].

The above or similar figures could give some order of magnitude idea useful for comparison purposes, however, the available information indicates that mechanical properties of foams are very sensitive to foam density, direction of cell-rise versus direction of loading, and test method.

All organic materials tested to date behave in a viscoelastic manner. Strictly speaking the thermal stresses caused on these materials by differential expansions or contractions cannot be expressed in terms of the standard modulus of elasticity and the free contraction constant.

Test methods have been devised to measure the thermal stress-thermal strain ratio (thermoelastic modulus) and the thermoelastic contraction as a function of temperature (Schroeder (1973) [60]). The main objection of such type of data is that because of the nonlinearity of the phenomenon it is not easy to superpose thermally induced and mechanically induced stresses. For example, tests reveal that the thermoelastic strain of a loaded specimen is not the same as that corresponding to the unloaded or free shrink specimen.

One way to circumvent these difficulties and still generate data which would be useful for engineering purposes, is to neglect non-linear effects, which at low temperatures seems to be justified, as was mentioned in connection with Figure 4-10 and is confirmed later, and to obtain mechanical property data using normal widely used test techniques, with the obvious additions to reproduce the required low temperature environment and to minimize thermally induced stresses.

Documents
Document Sharing Hub
Full document details: PD CEN/CLC/TR 17603-31-07:2021

A collection of data generated by US National Bureau of Standards is presented in Table 4-3 to Table 4-8 and Figure 4-13 to Figure 4-18 below. These data concern both tensile and compressive strengths. The main results of these tests can be summarized as follows:

1. The Modulus of Elasticity, yield strength, and ultimate strength increase with decreasing temperature, while the elongation decreases, Table 4-4 and Table 4-8 below.
2. The Modulus of Elasticity is twice as great in tension compared to compression, but the difference diminishes at lower temperatures. Compare Figure 4-14 and Figure 4-17 below.
3. Most foams become brittle at low temperatures, whereas the ductility is considerable at 195 K and above (Figure 4-13 and Figure 4-16 below). On the average, polystyrene foams are more ductile than polyurethanefoams at 76 K (Figure 4-16 below).
4. The Modulus of Elasticity and the strength, both tensile and compressive, are approximately linearly dependent on density. At low temperatures the density dependence is greater (Figure 4-14, Figure 4-15, and Figure 4-17, Figure 4-18 below). In the compressive case there is a minimum density below which the rigid foam cannot withstand any applied compressive force at low temperatures; by extrapolation of the straight lines corresponding to circle and inverted triangle data points in Figure 4-17 below, one obtains a zero value of E at finite density.
5. Specimens loaded along the rise are stronger than those loaded transversally to rise (Figure 4-13 and Figure 4-16 below). In the compressive case this is not necessarily true; notice, for instance, the foam YR-1 in Figure 4-16 below.
6. At most densities there is considerable data spread which can be attributed to foam components, manufacturing process, and blowing agent.

Table 4-3: Characterization of Foams Whose Properties Will Be Given Later

	Sample [a]	Type [b]	Density, ρ [kg.m^{-3}]	Polyol Component	Isocyanate Component [c]	Blowing Agent	Flame Retardant
Flexible	AF-1	PU	34,8	Polyether	TDI	All CO_2	No
	BF-4	PU	125	Polyether	PAPI/TDI		No
	BF-5	PU	123	Polyether	PAPI/TDI		No
	BF-6	PU	116	Polyether	PAPI/TDI		No
	CF-7	PU	33,8	Polyester	TDI		No
	CF-8	PU	32,7	Polyester	TDI		No
	CF-9	PU	33,5	Polyester	TDI		No
	DF-1	PU	110	Polyester	TDI		No
	DF-2	PU	111	Polyester	TDI		No
	DF-3	PU	105	Polyester	TDI		No
Rigid	JR-1	PU	66,2	Polyether	PAPI Prepol	CO_2 and	Yes
	KR-1	PU	30,6	Polyether	PAPI Prepol	Freon 11	Yes
	LR-3	PU	42,4	Polyether	TDI Prepol	CO_2 and	No
	MR-1	PU	68,4	Polyether	TDI Prepol	Freon 11	No
	NR-1	PU	95,6	Polyether	TDI Prepol	CO_2	No
	OR-1	PU	47,6	Polyester	TDI Prepol	CO_2	No
	OR-2	PU	47,7	Polyester	TDI Prepol	CO_2	No
	PR-1	PU	48,1	Polyether	PAPI	Freon 11	No

Documents
Document Sharing Hub
Full document details: PD CEN/CLC/TR 17603-31-07:2021

	Sample [a]	Type [b]	Density, ρ [kg.m^{-3}]	Polyol Component	Isocyanate Component [c]	Blowing Agent	Flame Retardant
	SR-2	PU	47,7	Polyether	PAPI	Freon 11	Yes
	TR-2	PU	32,4	Polyester	TDI Prepol	Freon 11	No
	UR-2	PU	43,6	Polyester	TDI Prepol	Freon 11	No
	VR-2	PU	61,0	Polyester	TDI Prepol	CO_2	No
	WR-2	PU	87,8	Polyester	TDI Prepol	CO_2	No
	XR-3	PU	48,2	Polyether	TDI Prepol	CO_2	No
	XR-4	PU	47,6	Polyether	TDI Prepol	CO_2	No
	YR-1	PS	52,2	Polystyrene	-	CO_2	No
	ZR-1	PS	100	Polystyrene	-	CO_2	No
						Pentane	
						Pentane	

[a] Material source: AF-1 to SR-2: CPR Division, Upjohn Company; TR-2 to Zr-1: Bendix Corporation

[b] PU: Polyurethane foam; PS: Polystyrene foam.

[c] TDI: Tolylene diisocyanate; PAPI: Polymethylene polyphenylisocyanate, registered trade name of Upjohn Co.; Prepol: Prepolymerized.

NOTE From Reed, Arvidson & Durcholz (1972) [52].

Table 4-4: Average Tensile Data of Polyurethane and Polystyrene Foams

Data at T = 76 K	Table 4-5
Data at T = 195 K	Table 4-6
Data at T = 300 K	Table 4-7

NOTE From Reed, Arvidson & Durcholz (1972) [52].

Documents
Document Sharing Hub
Full document details: PD CEN/CLC/TR 17603-31-07:2021

Table 4-5: Average Tensile Data of Polyurethane and Polystyrene Foams at $T = 76$ K T: Transverse; L: Longitudinal

Foam	Density, ρ [kg.m^{-3}]	Type [a]	Modulus of Elasticity, Ex10^{-6} [Pa]		Proportional limit σx10^{-5} [Pa]		Yield [b] strength, σ_0x10^{-5} [Pa]		Compressive strength, σx10^{-5} [Pa]		Elongation %			
											Plastic		Total	
			T	L	T	L	T	L	T	L	T	L	T	L
KR-1	30,6	PUR	12,5	-	3,2	-	-	-	3,7	-	0,06	-	3,05	-
KR-1	29,5	PUR	-	18,2	-	1,4	-	-	-	4,6	-	0,03	-	1,81
TR-2	32,4	PUR	20,4	-	3,0	-	-	-	3,6	-	0,03	-	1,80	-
LR-3	42,4	PUR	38,5	-	6,8	-	-	-	8,3	-	0,04	-	1,86	-
UR-2	43,6	PUR	33,4	-	4,7	-	-	-	6,0	-	0,01	-	1,88	-
UR-2	44,5	PUR	-	27,1	-	4,1	-	-	-	6,1	-	0,07	-	2,40
XR-4	47,6	PUR	31,7	-	-	-	-	-	5,6	-	0,00	-	1,77	-
OR-1	47,7	PUR	37,0	-	-	-	-	-	10,1	-	0,00	-	2,72	-
OR-1	46,3	PUR	-	45,0	-	-	-	-	-	6,3	-	0,00	-	2,03
SR-2	47,7	PUR	38,7	-	-	-	-	-	6,6	-	0,00	-	1,67	-
PR-1	47,7	PUR	32,8	-	5,0	-	-	-	5,4	-	0,02	-	1,70	-
VR-2	61,0	PUR	51,0	-	6,3	-	-	-	9,2	-	0,02	-	1,62	-
JR-1	64,6	PUR	40,4	-	-	-	-	-	7,9	-	0,00	-	1,93	-
MR-1	68,2	PUR	44,5	-	6,5	-	-	-	9,4	-	0,05	-	2,17	-
WR-2	87,8	PUR	63,0	-	11,0	-	-	-	14,4	-	0,05	-	2,22	-
NR-1	95,6	PUR	95,8	-	14,4	-	-	-	18,5	-	0,04	-	1,98	-
NR-1	94,8	PUR	-	85,4	-	13,2	-	-	-	15,7	-	0,06	-	2,21
CF-7	33,8	PUF	16,5	-	1,9	-	2,7	-	4,4	-	1,79	-	4,63	-
CF-7	32,5	PUF	-	17,6	-	2,6	-	3,7	-	4,9	-	0,83	-	3,54
AF-1	34,8	PUF	15,4	-	2,0	-	2,8	-	4,2	-	2,40	-	5,35	-
DF-1	108	PUF	102,7	-	6,6	-	12,3	-	26,3	-	3,27	-	5,90	-
BF-4	124	PUF	120,1	-	7,8	-	-	-	10,4	-	0,08	-	0,73	-
YR-1	52,2	PSR	57,4	-	7,2	-	9,9	-	11,2	-	0,72	-	2,02	-
YR-1	51,3	PSR	-	50,4	-	6,5	-	9,4	-	10,9	-	0,83	-	2,95
ZR-1	101	PSR	108,2	-	11,8	-	19,2	-	22,5	-	0,76	-	2,18	-

[a] PUR: polyurethane rigid; PUF: polyurethane flexible; PSR: polystyrene rigid.

[b] At 0,2% offset.

NOTE COMMENTS: 1) The rigid foam samples were cylindrical, 2,866x10^{-2} m in diameter and 7,62x10^{-2} m long. Specimens having a reduced middle subclause 6.21x10^{-2} m in diameter and 2,54x10^{-2} m long m in side and 7,62x10^{-2} m long. The specimens were epoxied to polycarbonate grips. Polycarbonate was chosen because its thermal expansion matched that of the adhesive at low temperature.
2) The rate of head movement of the testing machine was 5x10^{-4} m.min^{-1}.

Documents
Document Sharing Hub
Full document details: PD CEN/CLC/TR 17603-31-07:2021

3) Each value represents the average of about four tests. Strength data variation from the reported average were ± 10%. Suggested inaccuracies of the reported average strength data are ± 5%. Average elongation data are supposed to be inaccurate to ± 5%, and data variations from the reported averages are ± 10%. For a given test individual strength and elongation measurements are thought to be accurate to ± 1%.

NOTE From Reed, Arvidson & Durcholz (1972) [52].

Table 4-6: Average Tensile Data of Polyurethane and Polystyrene Foams at T = 195 K T: Transverse; L: Longitudinal

Foam	Density, ρ [kg.m^{-3}]	Type [a]	Modulus of Elasticity, Ex10^{-6} [Pa]		Proportional limit σx10^{-5} [Pa]		Yield [b] strength, σx10^{-5} [Pa]		Compressive strength, σx10^{-5} [Pa]		Elongation %			
											Plastic		Total	
			T	L	T	L	T	L	T	L	T	L	T	L
KR-1	30,6	PUR	10,1	-	2,2	-	2,6	-	3,2	-	0,88	-	4,01	-
KR-1	30,6	PUR	-	11,2	-	1,04	-	2,1	-	4,0	-	1,98	-	5,69
UR-2	39,2	PUR	11,9	-	2,6	-	4,1	-	6,1	-	0,96	-	6,10	-
UR-2	42,0	PUR	-	15,9	-	4,6	-	6,1	-	6,8	-	0,12	-	4,40
OR-1	47,1	PUR	14,5	-	3,8	-	7,5	-	8,1	-	0,16	-	5,70	-
NR-1	95,8	PUR	38,7	-	6,2	-	10,5	-	17,1	-	1,15	-	5,57	-
NR-1	94,3	PUR	-	45,2	-	6,3	-	11,4	-	17,4	-	1,14	-	4,03
CF-7	32,2	PUF	3,7	-	0,74	-	1,2	-	3,2	-	34,30	-	45,55	-
CF-7	33,6	PUF	-	6,9	-	1,1	-	1,7	-	3,7	-	23,7	-	28,9
YR-1	51,7	PSR	35,0	-	4,5	-	6,8	-	8,8	-	2,81	-	4,91	-
YR-1	50,6	PSR	-	30,2	-	3,2	-	6,4	-	8,7	-	1,83	-	3,92

[a] PUR: polyurethane rigid; PUF: polyurethane flexible; PSR: polystyrene rigid.

[b] At 0,2% offset.

NOTE COMMENTS: 1) The rigid foam samples were cylindrical, 2,866x10^{-2} m in diameter and 7,62x10^{-2} m long. Specimens having a reduced middle subclause 6.21x10^{-2} m in diameter and 2,54x10^{-2} m long m in side and 7,62x10^{-2} m long. The specimens were epoxied to polycarbonate grips. Polycarbonate was chosen because its thermal expansion matched that of the adhesive at low temperature.
2) The rate of head movement of the testing machine was 5x10^{-4} m.min^{-1}.
3) Each value represents the average of about four tests. Strength data variation from the reported average were ± 10%. Suggested inaccuracies of the reported average strength data are ± 5%. Average elongation data are supposed to be inaccurate to ± 5%, and data variations from the reported averages are ± 10%. For a given test individual strength and elongation measurements are thought to be accurate to ± 1%.

NOTE From Reed, Arvidson & Durcholz (1972) [52].

Documents
Document Sharing Hub
Full document details: PD CEN/CLC/TR 17603-31-07:2021

Table 4-7: Average Tensile Data of Polyurethane and Polystyrene Foams at T = 300 KT: Transverse; L: Longitudinal

Foam	Density, ρ [kg.m^{-3}]	Type [a]	Modulus of Elasticity, Ex10^{-6} [Pa]		Proportional limit σx10^{-5} [Pa]		Yield [b] strength, σx10^{-5} [Pa]		Compressive strength, σx10^{-5} [Pa]		Elongation %			
											Plastic		Total	
			T	L	T	L	T	L	T	L	T	L	T	L
KR-1	30,8	PUR	5,6	-	1,03	-	1,3	-	2,9	-	4,84	-	9,96	-
UR-2	40,0	PUR	16,1	-	1,0	-	2,4	-	5,0	-	2,86	-	5,89	-
UR-2	41,2	PUR	-	13,7	-	1,5	-	2,6	-	4,9	-	2,42	-	6,02
OR-1	47,3	PUR	17,2	-	2,4	-	3,7	-	5,4	-	1,57	-	4,35	-
NR-1	94,7	PUR	26,4	-	3,7	-	6,1	-	10,8	-	3,09	-	7,05	-
NR-1	94,7	PUR	-	31,0	-	3,4	-	6,3	-	10,4	-	2,00	-	5,68
CF-7	33,0	PUF	0,12	-	0,20	-	0,28	-	0,73	-	37,25	-	96,27	-
CF-7	33,2	PUF	-	0,19	-	1,6	-	0,28	-	0,85	-	35,33	-	82,03
YR-1	50,8	PSR	36,1	-	3,0	-	6,2	-	8,2	-	2,84	-	5,24	-
YR-1	50,9	PSR	-	38,7	-	3,9	-	6,3	-	8,3	-	2,10	-	4,20

[a] PUR: polyurethane rigid; PUF: polyurethane flexible; PSR: polystyrene rigid.

[b] At 0,2% offset.

NOTE COMMENTS: 1) The rigid foam samples were cylindrical, 2,866x10^{-2} m in diameter and 7,62x10^{-2} m long. Specimens having a reduced middle subclause 6.21x10^{-2} m in diameter and 2,54x10^{-2} m long m in side and 7,62x10^{-2} m long. The specimens were epoxied to polycarbonate grips. Polycarbonate was chosen because its thermal expansion matched that of the adhesive at low temperature.
2) The rate of head movement of the testing machine was 5x10^{-4} m.min^{-1}.
3) Each value represents the average of about four tests. Strength data variation from the reported average were ± 10%. Suggested inaccuracies of the reported average strength data are ± 5%. Average elongation data are supposed to be inaccurate to ± 5%, and data variations from the reported averages are ± 10%. For a given test individual strength and elongation measurements are thought to be accurate to ± 1%.

NOTE From Reed, Arvidson & Durcholz (1972) [52].

Table 4-8: Average Compressive Data of Polyurethane and Polystyrene Foams

Data at T = 76 K	Table 4-9
Data at T = 195 K	Table 4-10
Data at T = 300 K	Table 4-11

NOTE Individual strength and elongation measurements are accurate to ± 1%. Reported strength and elongation measurements are thought to be accurate to ± 7%, with the principal contributor to test inaccuracy being material inconsistency.

NOTE From Arvidson, Durcholz & Reed (1972) [4].

Documents
Document Sharing Hub
Full document details: PD CEN/CLC/TR 17603-31-07:2021

Table 4-9: Average Compressive Data of Polyurethane and Polystyrene Foams at *T* = 76 K T: Transverse; L: Longitudinal

Foam	Density, ρ [kg.m^{-3}]	Type [a]	Modulus of Elasticity, Ex10^{-6} [Pa]		Proportional limit σx10^{-5} [Pa]		Yield [b] strength, σ_0x10^{-5} [Pa]		Compressive Strength [c], σx10^{-5} [Pa]		Elongation %			
											Plastic		Total	
			T	L	T	L	T	L	T	L	T	L	T	L
UR-2	47,6	PUR	29,4	-	4,0	-	5,1	-	6,3	-	0,41	-	2,58	-
PR-1	46,8	PUR	-	36,1	-	5,4	-	-	-	6,5	-	0,11	-	1,92
NR-1	48,4	PUR	13,6	-	2,3	-	3,8	-	6,2	-	2,69	-	7,32	-
CF-7	47,4	PUF	-	23,0	-	3,5	-	5,8	-	7,0	-	0,72	-	3,75
YR-1	94,8	PSR	67,8	-	11,3	-	-	-	14,8	-	0,04	-	2,39	-
ZR-1	95,6	PSR	-	81,7	-	10,8	-	-	-	14,2	-	0,13	-	1,87
	34,1		12,0	-	2,1	-	2,8	-	3,0	-	0,35	-	2,88	-
	31,7		-	10,9	-	2,2	-	3,2	-	3,4	-	0,45	-	3,55
	51,6		31,6	-	3,7	-	5,0	-	5,4	-	3,28	-	5,02	-
	51,3		-	32,4	-	3,7	-	4,6	-	5,1	-	4,65	-	6,28
	99,5		73,8	-	9,3	-	13,7	-	15,1	-	0,58	-	2,32	-
	99,2		-	74,8	-	9,4	-	13,2	-	14,5	-	0,95	-	2,93

[a] PUR: polyurethane rigid; PUF: polyurethane flexible; PSR: polystyrene rigid.

[b] At 0,2% offset.

[c] Tests in which the stress continued to increase as the test progressed (i.e., the material did not exhibit an ultimate) were concluded at 10% total elongation. The corresponding values are in parentheses.

NOTE COMMENTS: 1) The rigid foam samples were cylindrical, 2,866x10^{-2} m in diameter and 2,54x10^{-2} m long. Flexible specimens were machined into a cube geometry with the length of each side equal to 2,54x10^{-2} m.
2) The rate of head movement of the testing machine was 5x10^{-4} m.min^{-1}.
3) Each value represents the average of at least three tests. The average strength deviations for a given type and loading direction were ± 9%, while the average elongation deviations were ± 8%. Individual strength and elongation measurements are accurate to ± 1%. Reported strength and elongation measurements are thought to be accurate to ± 7%, with the principal contributor to test inaccuracy being material inconsistency.

NOTE From Arvidson, Durcholz & Reed (1972) [4].

Documents Document Sharing Hub

Full document details: PD CEN/CLC/TR 17603-31-07:2021

Table 4-10: Average Compressive Data of Polyurethane and Polystyrene Foams at T = 195 K T: Transverse; L: Longitudinal

Foam	Density, ρ [kg.m^{-3}]	Type [a]	Modulus of Elasticity, Ex10^{-6} [Pa]		Proportional limit σx10^{-5} [Pa]		Yield [b] strength, σx10^{-5} [Pa]		Compressive Strength [c], σx10^{-5} [Pa]		Elongation %			
											Plastic		Total	
			T	L	T	L	T	L	T	L	T	L	T	L
UR-2	43,9	PUR	12,6	-	1,7	-	2,6	-	3,8	-	1,84	-	4,91	-
NR-1	41,3	PUR	-	11,2	-	1,7	-	2,3	-	3,4	-	2,35	-	5,59
CF-7	94,2	PUF	40,4	-	4,1	-	7,0	-	(11.6)	-	7,10	-	10,00	-
YR-1	94,5	PSR	-	51,4	-	4,6	-	7,3	-	(11.7)	-	7,68	-	10,00-
	33,3		2,0	-	0,33	-	0,57	-	(0.84)	-	5,96	-	10,00	5,43
	32,0		-	3,5	-	0,72	-	0,99	-	1,19	-	1,87	-	-
	51,3		23,6	-	3,2	-	4,1	-	(5.2)	-	7,80	-	10,00	10,00
	51,4		-	21,5	-	3,0	-	3,8	-	(4.8)	-	7,70	-	

[a] PUR: polyurethane rigid; PUF: polyurethane flexible; PSR: polystyrene rigid.

[b] At 0,2% offset.

[c] Tests in which the stress continued to increase as the test progressed (i.e., the material did not exhibit an ultimate) were concluded at 10% total elongation. The corresponding values are in parentheses.

NOTE COMMENTS: 1) The rigid foam samples were cylindrical, 2,866x10^{-2} m in diameter and 2,54x10^{-2} m long. Flexible specimens were machined into a cube geometry with the length of each side equal to 2,54x10^{-2} m.
2) The rate of head movement of the testing machine was 5x10^{-4} m.min^{-1}.
3) Each value represents the average of at least three tests. The average strength deviations for a given type and loading direction were ± 9%, while the average elongation deviations were ± 8%.
Individual strength and elongation measurements are accurate to ± 1%. Reported strength and elongation measurements are thought to be accurate to ± 7%, with the principal contributor to test inaccuracy being material inconsistency.

NOTE From Arvidson, Durcholz & Reed (1972) [4].

Documents
Document Sharing Hub
Full document details: PD CEN/CLC/TR 17603-31-07:2021

Table 4-11: Average Compressive Data of Polyurethane and Polystyrene Foams at T = 300 K T: Transverse; L: Longitudinal

Foam	Density, ρ [kg.m^{-3}]	Type [a]	Modulus of Elasticity, Ex10^{-6} [Pa]		Proportional limit σx10^{-5} [Pa]		Yield [b] strength, σ_0x10^{-5} [Pa]		Compressive strength [c], σx10^{-5} [Pa]		Elongation %			
											Plastic		Total	
			T	L	T	L	T	L	T	L	T	L	T	L
UR-2	46,3	PUR	7,0	-	1,3	-	1,9	-	3,0	-	3,26	-	7,62	-
NR-1	40,8	PUR	-	7,2	-	1,4	-	2,2	-	3,0	-	2,04	-	6,34
CF-7	95,1	PUF	17,2	-	3,5	-	5,2	-	8,0	-	3,27	-	7,93	-
YR-1	93,2	PSR	-	20,2	-	4,3	-	5,9	-	8,1	-	3,27	-	7,38
	33,3		0,06	-	0,021	-	0,024	-	(0.035)	-	4,13	-	10,00	-
	33,3		-	0,20	-	0,014	-	0,021	-	(0.04)	-	7,31	-	10,00
	51,9		19,8	-	3,4	-	3,7	-	(4.0)	-	7,94	-	10,00	-
	51,1		-	19,1	-	2,3	-	3,2	-	3,4	-	0,68	-	2,46

[a] PUR: polyurethane rigid; PUF: polyurethane flexible; PSR: polystyrene rigid.

[b] At 0,2% offset.

[c] Tests in which the stress continued to increase as the test progressed (i.e., the material did not exhibit an ultimate) were concluded at 10% total elongation. The corresponding values are in parentheses.

NOTE COMMENTS: 1) The rigid foam samples were cylindrical, 2,866x10^{-2} m in diameter and 2,54x10^{-2} m long. Flexible specimens were machined into a cube geometry with the length of each side equal to 2,54x10^{-2} m.
2) The rate of head movement of the testing machine was 5x10^{-4} m.min^{-1}.
3) Each value represents the average of at least three tests. The average strength deviations for a given type and loading direction were ± 9%, while the average elongation deviations were ± 8%.
Individual strength and elongation measurements are accurate to ± 1%. Reported strength and elongation measurements are thought to be accurate to ± 7%, with the principal contributor to test inaccuracy being material inconsistency.

NOTE From Arvidson, Durcholz & Reed (1972) [4].

Documents
Document Sharing Hub
Full document details: PD CEN/CLC/TR 17603-31-07:2021

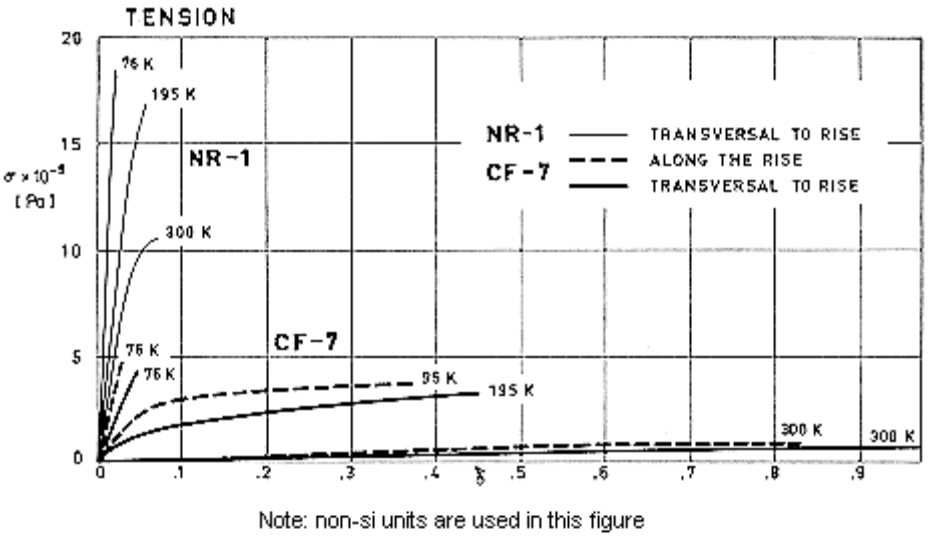

Figure 4-13: Tensile stress, σ, vs. strain, δ, for several polyurethane foams at 76, 195 and 300 K.

From Reed, Arvidson & Durcholz (1972) [52].

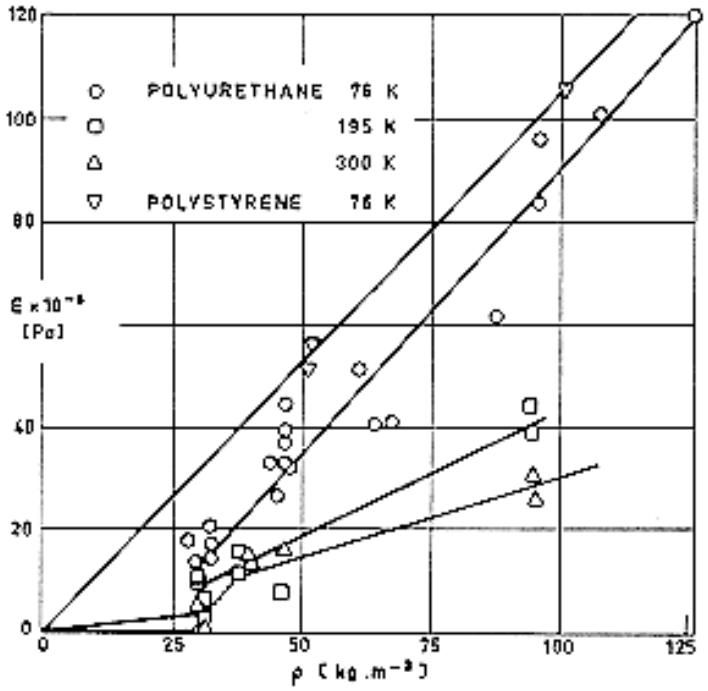

Figure 4-14: Modulus of Elasticity-tensile-*E*, as a function of density, ρ, for several organic foams.

Solid lines show the estimated dependence of *E* on foam density; dashed lines indicate transition between rigid foams (large *E*) and flexible foams (small *E*). From Reed et al. (1972) [52].

Documents
Document Sharing Hub
Full document details: PD CEN/CLC/TR 17603-31-07:2021

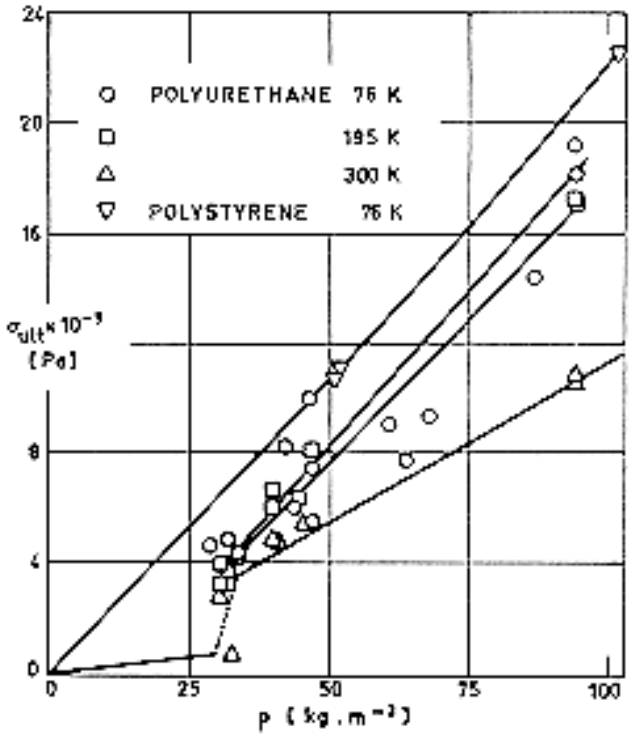

Figure 4-15: Ultimate tensile strength, σ_{ult}, as a function of density, ρ, for several organic foams.

Solid and dashed lines have the same meaning as in Figure 4-8. From Reed et al. (1972) [52].

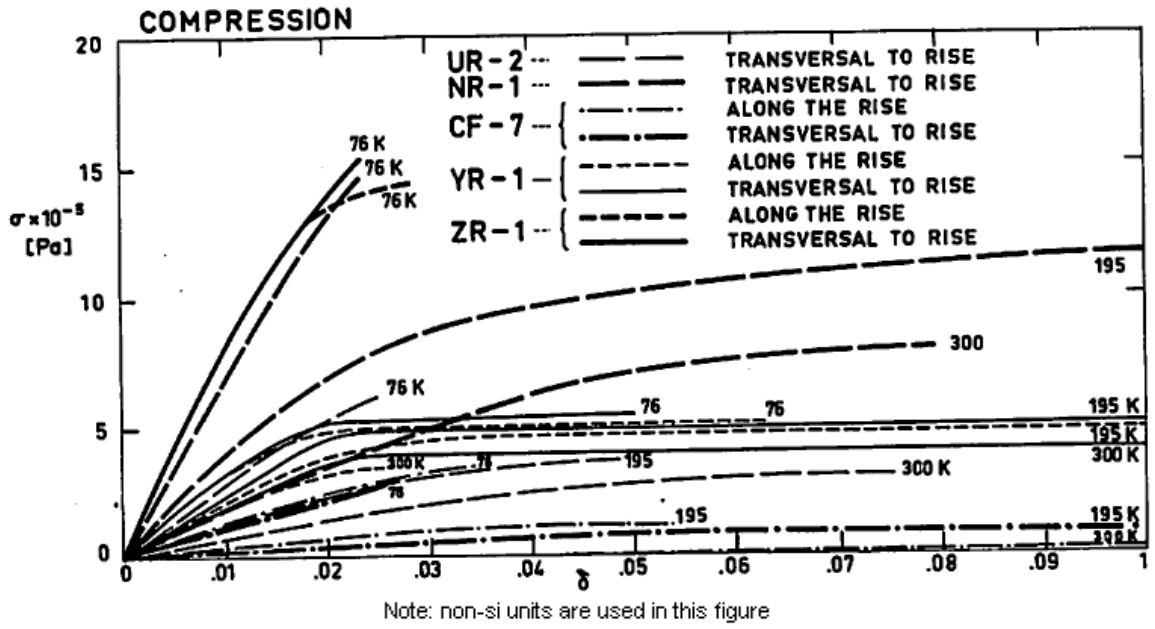

Figure 4-16: Compressive stress, s, vs, strain, d, for several organic foams at 76, 195 and 300 K.

From Arvidson, Durcholz & Reed (1972) [4].

Documents
Document Sharing Hub
Full document details: PD CEN/CLC/TR 17603-31-07:2021

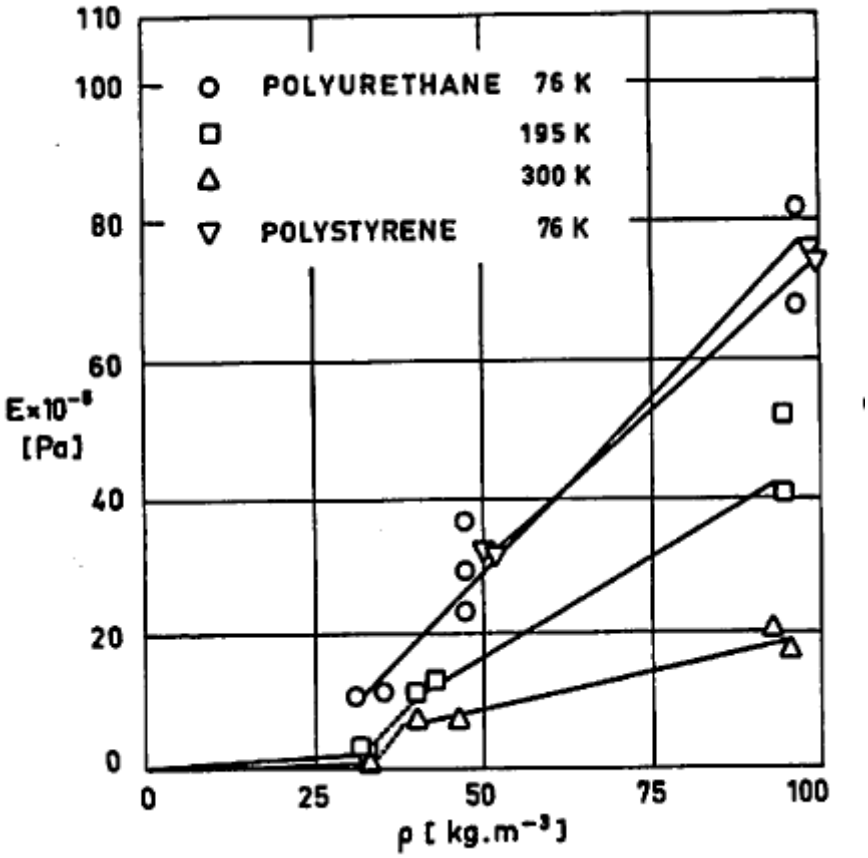

Figure 4-17: Modulus of Elasticity-tensile-*E*, as a function of density, ρ, for several organic foams.

Solid lines show the estimated dependence of *E* on foam density; dashed lines indicate transition between rigid foams (large *E*) and flexible foams (small *E*). From Arvidson et al. (1972) [4].

Documents
Document Sharing Hub
Full document details: PD CEN/CLC/TR 17603-31-07:2021